Harmful Algae 134 (2024) 102627

Contents lists available at ScienceDirect

Harmful Algae

journal homepage: www.elsevier.com/locate/hal

Spatio-temporal connectivity of a toxic cyanobacterial community and its associated microbiome along a freshwater-marine continuum

Océane Reignier [a], Myriam Bormans [b], Fabienne Hervé [c], Elise Robert [a], Véronique Savar [c], Simon Tanniou [c], Zouher Amzil [c], Cyril Noël [d], Enora Briand [a,*]

[a] IFREMER, PHYTOX, Laboratoire GENALG, Nantes F-44000, France
[b] UMR CNRS 6553 ECOBIO, University of Rennes 1, Rennes F-35042, France
[c] IFREMER, PHYTOX, Laboratoire METALG, Nantes F-44000, France
[d] IFREMER, IRSI – Service de Bioinformatique (SeBiMER), Plouzané, France

ARTICLE INFO

Editor: Edited by Dr Anusuya Willis

Keywords:
Microcystis bloom
Salinity
Cyanosphere
Microcystins
Osmolytes

ABSTRACT

Due to climate changes and eutrophication, blooms of predominantly toxic freshwater cyanobacteria are intensifying and are likely to colonize estuaries, thus impacting benthic organisms and shellfish farming representing a major ecological, health and economic risk. In the natural environment, *Microcystis* form large mucilaginous colonies that influence the development of both cyanobacterial and embedded bacterial communities. However, little is known about the fate of natural colonies of *Microcystis* by salinity increase. In this study, we monitored the fate of a *Microcystis* dominated bloom and its microbiome along a French freshwater-marine gradient at different phases of a bloom. We demonstrated changes in the cyanobacterial genotypic composition, in the production of specific metabolites (toxins and compatible solutes) and in the heterotrophic bacteria structure in response to the salinity increase. In particular *M. aeruginosa* and *M. wesenbergii* survived salinities up to 20. Based on microcystin gene abundance, the cyanobacteria became more toxic during their estuarine transfer but with no selection of specific microcystin variants. An increase in compatible solutes occurred along the continuum with extensive trehalose and betaine accumulations. Salinity structured most the heterotrophic bacteria community, with an increased in the richness and diversity along the continuum. A core microbiome in the mucilage-associated attached fraction was highly abundant suggesting a strong interaction between *Microcystis* and its microbiome and a likely protecting role of the mucilage against an osmotic shock. These results underline the need to better determine the interactions between the *Microcystis* colonies and their microbiome as a likely key to their widespread success and adaptation to various environmental conditions.

1. Introduction

Toxic cyanobacterial blooms are the most widespread harmful events in freshwater environments, increasing in frequency and intensity due to anthropogenic pressures, notably eutrophication and climate change (Erratt et al., 2023; O'Neil et al., 2012; Paerl et al., 2018; Rigosi et al., 2014). As a result, cyanobacterial blooms are a rapidly growing global threat to human and ecosystem health (Zhang et al., 2023). In the context of global change, the transfer of toxic freshwater cyanobacteria blooms to estuarine zones is set to intensify (Preece et al., 2017), jeopardizing ecological and economic resources estimated at over US$ 12, 600 billion per year (Costanza et al., 2014). These events are observed on a global scale (for review see Preece et al., 2017) and are becoming recurrent in the USA (*e.g.* San Francisco Estuary; Peacock et al., 2018), Australia (*e.g.* Swan River; Robson and Hamilton, 2003), Brazil (*e.g.* Patos Lagoon; De Souza et al., 2018), or even recently observed in France (Bormans et al., 2019). Most of the work published to-date indicate that the transfer of cyanobacteria is dominated by *Microcystis aeruginosa*, one of the freshwater cyanobacteria with the highest salinity tolerance (Black et al., 2011; Chen et al., 2015; Lewitus et al., 2008; Miller et al., 2010; Tonk et al., 2007; Verspagen et al., 2006). However, there are inter- and intraspecific variations in the ability of some *Microcystis* species/strains to acclimatize to increasing salinity gradients (Georges des Aulnois et al., 2019; Orr et al., 2004; Tonk et al., 2007). This halotolerance is thought to be partly linked to the production and accumulation of compatible solutes, such as sucrose and trehalose,

* Corresponding author.
E-mail address: enora.briand@ifremer.fr (E. Briand).

https://doi.org/10.1016/j.hal.2024.102627
Received 26 January 2024; Received in revised form 22 March 2024; Accepted 10 April 2024
Available online 18 April 2024

which help to balance intracellular and extracellular osmotic pressure (Georges des Aulnois et al., 2019; Georges des Aulnois et al., 2020; Hagemann, 2011; Sandrini et al., 2015; Tanabe et al., 2018). However, these results are laboratory-based experiments carried out on single-cell and monoclonal strains. Yet, in the natural environment, *Microcystis* forms large colonies surrounded by a thick mucilage made up of a complex of polysaccharides, nucleic acids, phospholipids and proteins (hereafter referred to as EPS for extracellular polymeric substances). EPS production by the cell is stimulated by environmental stresses (abiotic and/or biotic; for review see Kehr and Dittmann, 2015). By promoting cell aggregation and the formation of mucilaginous colonies, this morphological characteristic gives the population greater buoyancy in the water column, making them more accessible to light (Reynolds, 2007) and nutrients (Bonnet and Poulin, 2002), as well as providing physical protection against grazing (Fulton and Paerl, 1987) or to cope with osmotic shock (Bormans et al., 2023; Reignier et al., 2023). In addition to these benefits, colony formation provides a habitat for heterotrophic bacteria embedded in the mucilage. This microenvironment, known as the phycosphere (named by analogy with the rhizosphere; Bell and Mitchell, 1972), is the site of numerous biotic interactions such as competition or exchange of nutrients (Fuks et al., 2005; Yuan et al., 2009), inhibition (Ozaki et al., 2008; Rashidan and Bird, 2001) or stimulation of cyanobacterial growth (Casamatta and Wickstrom, 2000; Eiler et al., 2006; Jackrel et al., 2021), as well as biodegradation of cyanotoxins (Bourne et al., 2006; Briand et al., 2016) and the formation of aggregates (Shen et al., 2011). It has been shown that the structure and composition of bacterial communities associated with *M. aeruginosa* change during the development of a cyanobacterial bloom (Parveen et al., 2013), suggesting that the physiological state of cyanobacteria could have a direct impact on the community of associated bacteria. In addition, Penn et al. (2014), using a metatranscriptomic approach, highlighted the importance of the activity of bacteria associated with cyanobacteria in the metabolism of exudates produced and released by cyanobacteria, which could contribute to the maintenance of cyanobacterial growth by recycling carbon and nutrients. Finally, Zhu et al. (2016) revealed structural and functional differences in bacterial communities associated with different genera of cyanobacteria, knowing that these genera exhibited contrasting functional capabilities, including in the production of secondary metabolites. Studies have indeed highlighted a positive correlation between the dynamics of toxic *Microcystis* genotypes and those of bacteria capable of degrading microcystins (MCs), suggesting a strong interaction between these two microbial communities (Lezcano et al., 2017; Zhu et al., 2016). Consequently, assessment of the *Microcystis* microbiome is essential for understanding the processes that govern cyanobacterial proliferation and their ability to thrive even under stressful conditions, notably during its transfer along the land-sea continuum.

During these transfers, cyanotoxins (*i.e.* microcystins) in their particulate and dissolved forms were also found in the water column (Peacock et al., 2018; Preece et al., 2017) and in sediment (Bormans et al., 2020; Bukaveckas et al., 2017; Umehara et al., 2012). In addition, contaminations of marine organisms were reported (*e.g.* fish and shellfish, Amzil et al., 2023; Gibble et al., 2016; Lance et al., 2021), representing a major ecological, health and economic risk. Nevertheless, the prediction of the potential toxicity of *Microcystis* populations is still difficult. This is partly due (i) to the relative abundance of toxic and nontoxic *Microcystis* cells within blooms (Kaebernick and Neilan, 2001; Rainer and Thomas, 2003; Yancey et al., 2022), whose abundance can vary in time and space according to their fitness in the local environment (Briand et al., 2009; Sabart et al., 2010), as well as (ii) to intracellular regulation of toxin production (Bashir et al., 2023).

Consequently, in situ monitoring of natural population of *Microcystis* along a freshwater-marine continuum would enable us to better assess the fate of the freshwater cyanobacteria, their toxins and their associated microbiome in the estuarine zone. We investigated the dynamics of the cyanobacterial population and its associated microbiome along a freshwater-marine continuum to determine (i) whether increasing salinity induces changes in composition (at population and genotype levels) and metabolism (osmolytes and cyanotoxins) of the cyanobacterial community, and (ii) to what extent these changes affect the associated microbiome. In particular we hypothesized that (1) *Microcystis aeruginosa* would be the most salt tolerant species, (2) that the proportion of potentially toxic species and toxic quotas would increase along the salinity gradient, (3) that an increase in compatible solutes would occur along the continuum as a response to the osmotic stress and (4) that the microbiome associated with the mucilage would be better conserved than in the surrounding water.

2. Material and methods

2.1. Study site and sampling strategy

The study site is a moderate length freshwater-marine continuum (< 10 km), located in the Morbihan (Brittany, France), from the Pen Mur freshwater reservoir upstream to the Pen Lan estuary and the marine outlet, through the Saint Eloi River. Freshwater releases from the Pen Mur reservoir into the estuary are frequently observed, leading to the transfer of cyanobacteria and cyanotoxins into the estuary (Bormans et al., 2019, 2020), contaminating mussels (Amzil et al., 2023) and estuary's sediments (Bormans et al., 2020).

During the summer of 2021, four stations along this freshwater-marine gradient were sampled. Two stations were in the freshwater section, F1 in the Pen Mur reservoir (47°33′45.0288″ N, 2°29′31.667″ W) and F2 in the St Eloi River downstream of the reservoir (47°33′16.045″ N, 2°29′18.207″ W), whereas E1 and E2 were located in the Pen Lan estuarine section (47°31′36.358″ N, 2°29′37.917″ W and 47°31′4.5084″ N, 2°29′55.3596 W). Sampling was performed at three separate times corresponding to the beginning (August 23, T0), middle (September 6, T1) and end (September 21, T2) of the cyanobacteria proliferation period observed in the freshwater reservoir (F1). To maximize the freshwater discharge and minimize the tidal contribution (tidal range between 4.3 and 4.6 m), we consistently sampled the downstream stations within 1 h of low tide. At each station, ten liters of surface water (depth 0.25 m) were filtered through a 500 μm net, then brought directly to the laboratory in the dark conditions at 4 °C, and processed for further analyses.

2.2. Physico-chemical parameters

Surface water temperature (°C) and salinity (practical salinity unit, PSU) were performed in situ with a portable HQ40d multi-parameter probe (Hach). Upon arrival at the laboratory, water sample aliquots (50 mL) were processed directly for turbidity (Formazin Nephelometric Unit, FNU; 21,000 N IS Turbidimeter™ Hach; following the International Organization of Standardization ISO method 7027) and pH (Mettler Toledo SevenEasy™ pH-meter). For Chloropyll *a* and dissolved nutrient concentrations (phosphate, nitrate and carbon), 150 mL of water sample aliquots were filtered through GF/F 0.7 μm filters (Whatman, Buckinghamshire, UK) in duplicate for each point. Filters and filtrates were stored at −20 °C until analysis. Chlorophyll *a* was extracted from filters using 90 % acetone for 12 h in the dark condition at 4 °C and analyzed by monochromatic spectrophotometry (Aminot and Kérouel, 2004). Dissolved phosphate and nitrate concentrations were measured in the filtrates according to common colorimetric methods (Aminot and Chaussepied, 1983) with a sequential Gallery analyser (Thermo Fisher). Phosphate concentration was measured with the method of Murphy and Riley (1962) and nitrate concentration was measured after reduction to nitrite on a cadmium-copper column (Henriksen and Selmer-Olsen, 1970). Dissolved organic carbon was measured with a high-temperature persulfate oxidation technology using an OI Analytical carbon analyzer (model 1010 with a 1051 auto-sampler; Bioritech, France) following the ISO method 8245 (ISO, 1999).

2.3. Phytoplankton diversity

The standard protocol for sampling, conservation, observation and counting of lake phytoplankton for application of the Water Framework Directive (Version 3.3.1) (Laplace-Treyture et al., 2009) was followed to sample, identify and quantify the phytoplankton diversity. Water sample aliquots (20 mL) were fixed with acidic Lugol's solution (1 % final concentration) and stored at 4 °C in the dark until analysis.

Species determination, based on morphological criteria using reference books (Bourelly, 1985; Komárek and Anagnostidis, 2008), and counts were performed at a magnification of × 320 with an inverted microscope (Zeiss Axio observer 5, Oberkochen, Germany). For each sample, photographs of the various taxa were taken to estimate their biovolumes and their reprocessing was done using Zen 2.3 software. Biovolumes were based on the geometrical estimation suggested by Sampognaro et al. (2020) for *Microcystis* species and Sun and Liu (2003) for the other taxa.

2.4. Chemical analysis of cyanotoxins and osmolytes by LC-MS/MS

2.4.1. Cyanotoxin analyses

As described in Bormans et al. (2019), 500 mL was filtered through a 1.2 μm GF/C glass filter (Whatman) to separate the cell pellet for the intracellular toxins and the filtrate for dissolved extracellular toxins. Both filters and filtrates were frozen at - 20 °C until chemical analysis.

For intracellular cyanotoxins extraction, filters were ground with 500 mg of glass beads (0.15–0.25 mm; VWR) and 4 mL of MeOH using a mixer mill (MM400; Retsch) for 30 min at 30 Hz. After centrifugation at 13 000 g for 5 min at 4 °C, 500 μL of supernatant were filtered through a 0.2-μm filter (Nanosep MF; Pall) and frozen until LC–MS/MS analysis.

For extracellular cyanotoxins extraction, filtrates were purified on a BondElut C18 SPE cartridge (Solid Phase Extraction; 200 mg - Agilent) according to the ISO 20,179 standard method (ISO, 2005). Methanolic extracts (V_{Final} = 4 mL) were also filtered through a 0.2-μm filter (Nanosep MF; Pall) and then frozen until LC–MS/MS analysis.

LC-MS/MS analysis was performed by Ultra Fast Liquid Chromatography (model UFLC, Nexera, Shimadzu) coupled to a triple-quadrupole mass spectrometer (5500 QTrap; ABSciex). Toxins were separated on a Kinetex XB-C18 column (2.6 μm; 100×2.1 mm; Phenomenex) with water (A) and acetonitrile (B), both containing 0.1 % formic acid [vol/vol] at 0.3 mL min^{-1} flow rate. The elution gradient was raised from 30 % to 80 % B in 5 min, and held during 1 min before dropping down during 0.5 min to the initial conditions. As described in Réveillon et al. (2024), mass spectrometry (MS/MS) detection was performed with electrospray ionization interface (ESI) in positive mode using multiple reaction monitoring (MRM) with two transitions per toxin (Table S1A). Nine certified microcystin (MC) standards (dmMC-RR, MC-RR, MC-YR, MC-LR, dmMC-LR, MC-LA, MC-LY, MC-LW, MC-LF; Novakits) and one nodularin standard (NOD; Novakits) were used to quantify the toxin concentration in both intracellular and extracellular fractions, using an external 6-point calibration curve (see Table S1B for the limit of detection and quantification in the methanolic extracts). Data acquisition and processing were performed using Analyst 1.7.2 (ABSciex) software.

2.4.2. Sugar and osmolyte analyses

Methanolic extracts prepared for toxin analysis (intracellular) were used for sugar and osmolytes analyses. Sample analyses were performed on a UFLC (model UFLC, Shimadzu) coupled to a triple-quadrupole mass spectrometer (4000 QTrap, ABSciex) equipped with a turboV® ESI source.

For sugar analysis, the chromatographic separation was performed on a BEH Amide column (1.7 μm, 150 × 2.1 mm, Waters) with a guard column (1.7 μm, 5 × 2.1 mm). The mobile phases were water (A) and acetonitrile (B). The flow rate was set at 0.25 mL min^{-1} and the injection volume was 5 μL. Column and sample temperatures were maintained at 35 °C and 4 °C, respectively. A gradient elution was used, starting with 78 % B, decreasing to 74 % B over 9 min, then decreasing in 0.1 min to 20 % B held for 3 min, then increasing to 78 % B in 0.1 min and held for 6 min to equilibrate the system. The LC-MS/MS system was used in negative ionization and multiple reaction monitoring (MRM) mode, with four transitions per compound. Negative acquisition experiments were optimized using the following source settings: curtain gas set at 20 psi, ion spray at −4000 V, temperature of 450 °C, gas 1 and 2 set at 40 and 50 psi, respectively, and an entrance potential of 10 V. The transitions and MS/MS parameters that were used are given in Table S2A. The most intense transition, giving the product ion *m/z* 58.9, was used to quantify sucrose and trehalose. Compound were quantified using external 5-point calibration curves of standards (sucrose from Sigma-Aldrich, trehalose from Acros Organic) solubilized in methanol, with concentrations from 10 nM to 1000 nM (see Table S2B for the limit of detection and quantification in the methanolic extracts).

For osmolytes (DMSP, betaine, methionine and proline) analysis, based on Curson et al. (2018), the chromatographic separation was performed with a Hypersil GOLD HILIC column (3 μm, 150 × 2.1 mm, Thermo Fisher Scientific) with a guard column (3 μm, 10 × 2.1 mm). The binary gradient consisted of water-acetonitrile (90/10 [vol/vol]) containing 4.5 mM ammonium formate (A) and water-acetonitrile (5/95 [vol/vol]) containing 5 mM ammonium formate (B). The flow rate was 0.25 mL min^{-1} and the injection volume was 5 μL. The column and sample temperatures were 30 °C and 4 °C, respectively. A gradient elution was used, starting with 90 % B during 1 min, then decreasing to 45 % B over 7 min, held for 4 min, then increasing to 90 % B in 0.1 min and held for 4 min to equilibrate the system. The LC-MS/MS system was used in positive ionization mode and MRM, with the two transitions per compounds. Acquisition experiments were set up using the following source settings: curtain gas set at 25 psi, ion spray at 5500 V, temperature of 550 °C, gas 1 and 2 set at 50 and 55 psi, respectively, and an entrance potential of 10 V. The transitions and MS/MS parameters that were used are given in Table S2A. The most intense transition was used to quantify the osmolytes. Compounds were quantified using external 5-point calibration curves of standards (Sigma-Aldrich) solubilized in methanol, with concentrations from 50 nM to 5000 nM (see Table S2B for the limit of detection and quantification in the methanolic extracts). Acquisition and data processing were performed using Analyst 1.7.2 (ABSciex) software.

2.5. Analysis of the bacterial community

2.5.1. DNA extraction

Water samples (100–500 mL) were sequentially filtered in duplicate through a 20 μm polycarbonate membrane filter (Whatman) to collect attached living bacterial communities and then, 100 mL of the filtrate was filtered through a 0.22 μm polycarbonate membrane filter (Whatman) to recover free-living bacterial communities. Filters were stored at −80 °C prior to DNA extraction. Genomic DNA from 20 to 0.22 μm polycarbonate filters was extracted using the NucleoSpin Plant II DNA extraction kit (Macherey Nagel) following instruction from the manufacturer. Briefly, in addition to the buffer solution, a solution of lysosyme (20 mg mL^{-1}; Sigma-Aldrich) and proteinase K (20 mg mL^{-1}; Macherey Nagel) was added to the crushed filters. Samples were vortexed and incubated for 2 h at 56 °C (900 rpm). The DNA extract was washed and purified before elution in a final volume of 100 μL of elution buffer. For each extract, the DNA purity and concentration were quantified by UV spectrometry (NanoDrop^{TM} 2000; Thermo Scientific), and then normalized to 10 ng μL^{-1}.

2.5.2. Quantification of potentially MC-producing microcystis cells and MC-degrading bacteria by real-time PCR

The proportion of *mcy* genotypes in the *Microcystis* population was determined by a real-time PCR analysis. Two target gene regions located on the chromosome (Tillett et al., 2000) were used : the intergenic spacer region within the phycocyanin (*PC*) operon and the *mcyB* region, which carries out one step in MC biosynthesis encoding for the Non-ribosomal peptide synthetases (NRPS) adenylation domain that is responsible for the recognition of one variable amino acid of the MC molecule (Mikalsen et al., 2003). The primers and probes used for the *PC* and *mcyB* genes are specific for *Microcystis* (Kurmayer and Kutzenberger, 2003), and have been described previously (Briand et al., 2009).

The MC-degrading bacterial community possessing the *mlr* gene cluster (Bourne et al., 2006) was quantified by a real-time PCR analysis using the targeted *mlrA* gene. The *mlrA* gene encodes for the first enzyme in the degradation of MC process by bacteria (Saito et al., 2003). The primers and probes used for the *mlrA* gene are those described previously by Lezcano et al. (2018).

Amplifications by real-time PCR was carried out using a CFX Opus Real-Time PCR system (BioRad). Each reaction mixture had a final volume of 20 µL, containing 1X QuantiTech Probe PCR Master Mix (Qiagen), 0.3/0.9/0.4 µM of primers (*PC/mcyB/mlrA* respectively), 0.1/0.25/0.2 µM of probe (*PC/mcyB/mlrA* respectively), and 1 µL of either a DNA standard or sample normalized to 10 ng μL^{-1}. Each sample was prepared in duplicate. Negative control without DNA was included for each PCR run. Thermal cycling conditions for gene amplification were performed with an initial activation step at 95 °C for 15 min, followed by 45 cycles of denaturation at 94 °C for 15 s and annealing/extension at 60 °C during 1 min for *mcyB* and *PC* genes, and at 62 °C during 1 min for *mlrA* gene. Acquisition and data processing were performed using CFX Maestro 2.2 software (BioRad).

For each run of samples, serial dilutions of genomic DNA from the MC-producing *Microcystis aeruginosa* strain PCC 7806 (from the Pasteur Culture Collection of Cyanobacteria, Paris, France; https://webext.pasteur.fr/cyanobacteria/) were used to generate standard curves for the quantification of the *mcyB* and *PC* genes. The standard curve for the *PC* was linear between 2.17×10^1 and 2.17×10^8 gene copies with a R^2 of 0.985 and an efficiency of 103 %. The standard curve for the *mcyB* gene was linear between 2.17×10^1 and 2.17×10^8 gene copies with a R^2 of 0.989 and an efficiency of 102 %. Serial dilutions of genomic DNA from the MC-degrading *Sphingopyxis* sp. strain IM-2 (kindly provided by Dr. Maria Angeles Lezcano, Centro de Astrobiologia, Madrid, Spain) was used to generate standard curve for the quantification of the *mlrA* gene. The standard curve for the *mlrA* gene was linear between 9.75×10^1 and 9.75×10^7 gene copies with a R^2 of 0.991 and an efficiency of 92 %. For the three genes, the number of gene copies per sample was calculated using the standard curve of the target gene copy number versus the threshold cycle (Ct) for each fraction. The total number of gene copies per sample was obtained by summing the number of gene copies per fraction (attached and free-living bacterial communities fractions).

2.5.3. Identification of the microbial consortium by 16S amplicon sequencing

The bacterial community was examined with primers targeting the V4-V5 hypervariable region of the 16S rRNA gene using universal primers assembled with the Illumina adapters : Forward (NGS-515F): 5′-CTT TCC CTA CAC GAC GCT CTT CCG ATC TGT GYC AGC MGC CGC GGT AA-3′, Reverse (NGS-926R): 5′-GGA GTT CAG ACG TGT GCT CTT CCG ATC TCC GYC AAT TYM TTT RAG TTT-3′ (412 bp) (Parada et al., 2016). Each PCR reaction, performed in triplicate, contained 10 ng of extracted DNA, 0.2 µM of each primer, 1X Taq polymerase (Phusion High-Fidelity PCR Master Mix with GC Buffer; Thermo Scientific) and DNA/RNAse free water for a total volume of 25 µL. The PCR cycle conditions included an initial denaturation step at 95 °C for 5 min, followed by a 32-cycle hybridization step at 95 °C for 30 s, 50 °C for 60 s and 72 °C for 60 s, ending with an elongation step at 72 °C for 5 min. No template control with nuclease-free water were performed to check contamination. PCR products quality and integrity were verified by gel electrophoresis (1 % agarose). Finally, the triplicate PCR products for each sample were pooled before sequencing. Secondary PCR amplification for the addition of the Illumina compatible sequencing adapters and unique per-sample indexes was conducted at GeT-PlaGe France Genomics sequencing platform (Toulouse, France). Barcoded amplicons were quantified, quality-checked, normalized, pooled, and sequenced within one sequencing run using the 2 × 250 paired-end method on an Illumina MiSeq instrument with a MiSeq Reagent Kit V3 chemistry (Illumina), according to the manufacturer's recommendations. The sequencing dataset was deposited in the European Nucleotide Archive (ENA) under the project number PRJEB70923.

Bioinformatic analyses of the raw data were performed using SAMBA (https://gitlab.ifremer.fr/bioinfo/workflows/samba; v4.0.0), a standardized and automatized metabarcoding workflow developed by the Ifremer Bioinformatics Platform (SeBiMER). SAMBA was developed using Nextflow (Di Tommaso et al., 2017) and consists of three main parts: data integrity checking, bioinformatics processes, and statistical analyses. This workflow is mainly based on the use of QIIME 2 (Bolyen et al., 2019) and DADA2 (Divisive Amplicon Denoising Algorithm) (Callahan et al., 2016) with default parameters (unless indicated). Briefly, primers were removed with removal of reads with incomplete or incorrect primer sequences using Cutadapt (Martin, 2011). Then, filtered reads were clustered into ASV (Amplicon Sequence Variants) using DADA2 following a four steps approach: quality filtering, sequencing error correction, ASV inference (pairwise read merging) and chimera detection. A complementary step of ASV clustering was performed using dbOTU3 (Olesen et al., 2017) allowing to counteract the identification of false-positive ASV (PCR biases, remaining sequencing errors). The generated ASVs were then taxonomically assigned using a Naive Bayesian method against the SILVA v138.1 database (Glöckner et al., 2017; Quast et al., 2012).

Statistical analyses of diversity were carried out on normalized data by applying the CSS method on the R phyloseq object generated by the SAMBA workflow. The alpha diversity was investigated using four indices: Chao1, Shannon, Simpson's inverse, and Pielou. Beta diversity analyses were achieved by ordination method using Non-metric multidimensional scaling (NMDS) with Bray-Curtis dissimilarity matrices (Lozupone and Knight, 2005). Linear discriminant analysis (LDA) effect size (LEfSe) was used to identify bacterial taxa that were significantly enriched along the freshwater-marine continuum. This analysis was performed using the default settings (alpha = 0.05, effect-size threshold of 2).

To identify and quantify the core microbiome, *i.e.* the bacterial taxa shared among stations and times in the attached fraction (and in all replicates) as defined by Neu et al. (2021), UpSetR package was used (Conway et al., 2017). All data and codes are available on gitlab (https://gitlab.com/oreignie/DEMISEL_field.git).

3. Results

3.1. Physico-chemical characteristics of the freshwater-marine continuum

The physico-chemical characteristics of the water sampled at each site and sampling time are presented in Table 1. Along the continuum for each time, water temperature was relatively constant (20 ± 2 °C), while salinity increased from upstream (0.1) to downstream (22). As the salinity gradient increased, nitrate concentrations decreased ($N—NO_3$ = 4.3 mg L^{-1} at F1 to 0.4 mg L^{-1} at E2), while phosphate concentrations remained consistently low ($P\text{-}PO_4$ < 0.14 mg L^{-1}). In the freshwater reservoir (F1), Chl *a* and pH, which can be used as an indicator of algal biomass, increased significantly during the bloom. These parameters presented on average an upstream to downstream decrease. Turbidity levels in the freshwater reservoir (F1) reached a peak of 831 FNU during the bloom and this high turbidity persisted along the freshwater-marine continuum, indicating a substantial presence of particulate organic matter. At the same time, DOC concentrations were higher in the freshwater reservoir than in the estuarine section, as well as being

Table 1
Physico-chemical parameters measured in the water at the four stations (F1, F2, E1, and E2) during pre-bloom, bloom and post-bloom campaigns.

Time	Station	Salinity	Water temperature (°C)	Turbidity (FNU)	pH	Chl*a* (µg L^{-1})	N-NO_3 (mg L^{-1})	P-PO_4 (mg L^{-1})	DOC (mg L^{-1})
Pre-bloom	**F1**	0.1	21	15	9.3	34.7	4.3	< 0.01	91.0
	F2	0.1	20	12	7.9	8.0	2.8	0.02	88.9
Bloom	**F1**	0.1	22	831	9.7	1321.7	2.1	0.14	21.2
	F2	0.1	22	117	7.7	24.0	2.4	0.01	4.1
	E1	8.0	21	40	7.4	11.6	1.6	0.04	16.2
	E2	22	22	39	7.7	3.6	0.4	0.07	11.8
Post-bloom	**F1**	0.1	19	16	8.3	50.7	2.3	< 0.01	5.9
	F2	0.1	19	16	7.7	45.4	1.6	< 0.01	3.6
	E1	5.3	18	54	7.7	6.2	0.6	0.02	4.8
	E2	20	18	73	7.7	12.5	0.4	0.04	3.1

higher during the bloom than during the post-bloom.

3.2. Phytoplankton biomass and community composition along the salinity gradient

The phytoplankton community sampled along the freshwater-marine continuum was strongly dominated by cyanobacteria (over 90 % in biovolume; Fig. 1). In particular, the cyanobacterial biomass was characterized by several species of *Microcystis* (*M. aeruginosa, M. wesenbergii, M. viridis, M. smithii, M. flos-aquae, M. firma, M. botrys*, and *Microcystis* sp. unicellular), accounting for a minimum of 55% of the total phytoplankton biovolume in F1 during the post-bloom.

During the pre-bloom, corresponding to 35 µg L^{-1} of Chl *a* in the freshwater reservoir (F1), the cyanobacterial community was dominated by *M. aeruginosa* with a concentration of 2.5×10^5 cells mL^{-1} (Table S3), while the cyanobacterial community was co-dominated in the river (F2) by *M. aeruginosa* and *M. wesenbergii* with an average concentration of ~3 $\times 10^5$ cells mL^{-1} (Table S3).

During the bloom, corresponding to 1322 µg L^{-1} of Chl *a* in the freshwater reservoir (F1), *M. aeruginosa* and *M. wesenbergii* co-dominated and represented more than 85 % in biovolume of the phytoplankton community in the freshwater section, with a maximum concentration at F1 of 9×10^6 and 2×10^7 cells mL^{-1} respectively (Table S3). In contrast, the estuarine section was characterized by low biomass values and a marked selection in the composition of the phytoplankton community. At E1, *M. aeruginosa* dominated the phytoplankton community, constituting over 80 % of the biovolume (corresponding to 2.4×10^5 cells mL^{-1}, Table S3). However, at E2, its dominance declined to approximately 45 % of the phytoplankton biovolume (5×10^3 cells mL^{-1}, Table S3). Concurrently, *M. botrys* became more prominent, representing about 55 % of the phytoplankton community biovolume (8.6×10^3 cells mL^{-1}, Table S3).

During the post-bloom, corresponding to 51 µg L^{-1} of Chl *a* in the freshwater reservoir (F1), a co-dominance of *M. aeruginosa, M. wesenbergii* and *Dolichospermum* was observed representing more than 80 % of the phytoplankton community (*i.e.* 5.8×10^4, 7.4×10^4 and 6.5×10^3 cells mL^{-1} respectively, Table S3) and ~90 % in the river at F2 (*i.e.* 3.6×10^5, 5.8×10^5 and 1.9×10^4 cells mL^{-1}, respectively, Table S3). In the estuarine section, characterized by low biomass values, *M. aeruginosa* was the dominant species accounting for ~50 % of the biovolume of the phytoplankton community (*i.e.* 6.2×10^4 and 5.3×10^4 cells mL^{-1} at E1 and E2, respectively, Table S3), followed by *M. wesenbergii* and *M. botrys* accounting for 20 % each at E1 (*i.e.* 1.8×10^4 cells mL^{-1}, Table S3) and by *M. wesenbergii* at E2 (*i.e.* 2.7×10^4 cells mL^{-1}, Table S3). *Dolichospermum* represented less than 6 % of the phytoplankton community (*i.e.* 5.2×10^2 and 8.8×10^1 cells mL^{-1} at E1 and E2, respectively, Table S3).

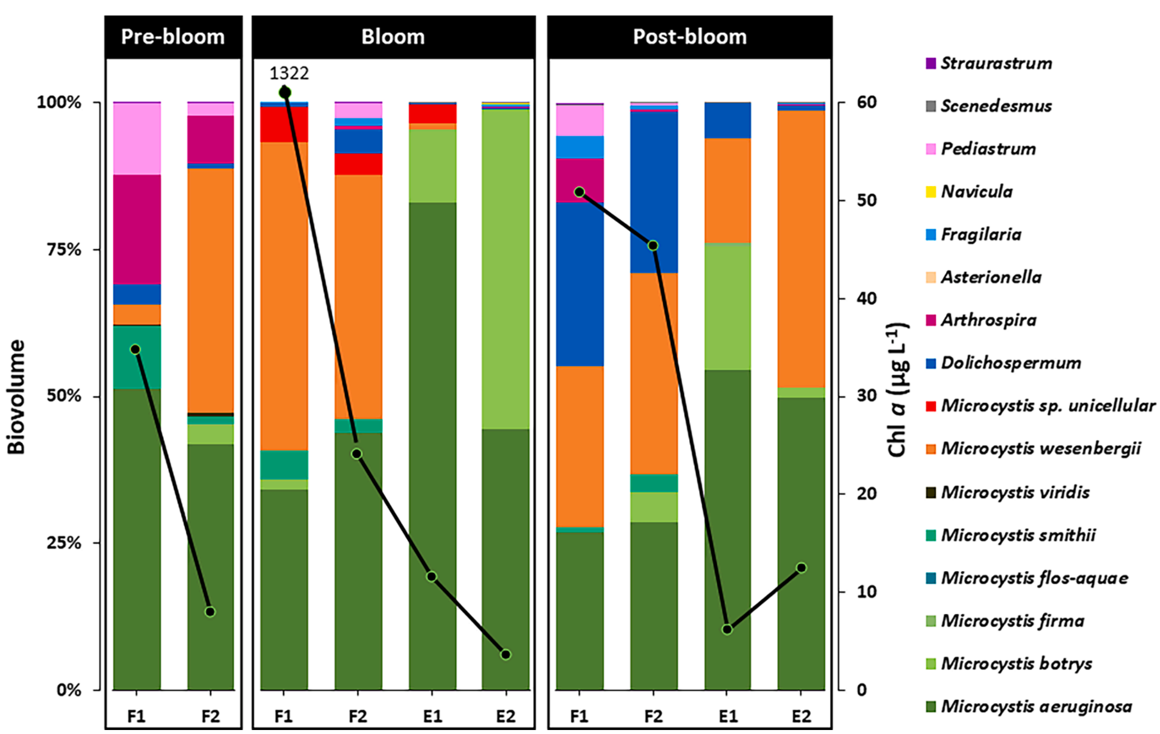

Fig. 1. Dynamic of the composition of phytoplankton community (histograms) expressed as biovolume proportions (see Table S3 for more details) and of Chlorophyll *a* concentration along the freshwater-marine continuum (F1, F2, E1, E2) during pre-bloom, bloom and post-bloom campaigns.

3.3. Spatio-temporal distribution of potentially MC-producing Microcystis

As the cyanobacterial population was mainly composed of *Microcystis* species, we monitored the dynamics of the relative abundance of potentially MC-producing *Microcystis* cells. The proportion of *Microcystis* cells potentially producing MCs was calculated by dividing the copy number of the *mcyB* gene (marker for potentially toxic *Microcystis* cells) by the copy number of the *PC* gene (marker for the total *Microcystis* population, i.e. toxic and nontoxic *Microcystis* cells) (Fig. 2). During the development of the bloom in the freshwater reservoir (F1), the relative abundance of *mcyB* gene decreased from ~64 % to 32 % at the pre-bloom and post-bloom respectively. For each sampling time, the relative abundance of *mcyB* gene increased along the freshwater-marine continuum, with the highest relative abundance observed at F2 (106 ± 3 %), E1 (90 ± 2 %) and E2 (44 ± 4 %) respectively at pre-bloom, bloom and post-bloom.

3.4. Intracellular and extracellular MC concentrations

The total concentration of MC observed during the study along the freshwater continuum averaged ~1 μg L^{-1} and was mostly measured in the intracellular form (Fig. 3A). As a result, calculated MC quota per *mcyB* gene copy were highly contrasted from freshwater to estuary sites with a 500-fold and a 2-fold increase from F1 to E2 during bloom and post-bloom periods respectively (Fig. 4). Six of the nine MC variants tested could be quantified in the cyanobacterial biomass during this study (Fig. 3B). While the MC-LR variant predominated by more than 75 % in the freshwater section during the pre-bloom, the toxin profiles were more diverse during bloom and post-bloom. For both sampling periods, the MC variants found averaged 40 % of MC-LR, 30 % of MC-YR, 10 % of MC-RR, 5 % of dmMC-LR, and less than 3 % of dmMC-RR during the bloom or less than 3 % of MC-LY in post-bloom samples. No particular selection of variants was observed along the continuum, except at E2 station during the post-bloom where only MC-LR was detected.

Concerning the extracellular MC concentration, a slight increase was observed along the freshwater-marine continuum during the post-bloom period (Fig. 3A). More specifically, four of the nine MC variants investigated (Fig. 3B) could be quantified in dissolved form in the water: MC-LR, dmMC-LR, MC-RR, and MC-YR. No particular selection of variants was observed in the water column along the freshwater-marine continuum, but two toxin profiles could be distinguished according to the bloom period. Indeed, before and during the bloom, the toxin profile averaged 90 % MC-LR, 8 % dmMC-LR and 2 % MC-RR. However, in the post-bloom period from F2 to E2, the proportion of MC-LR reduced by half, accounting for only 45 % of the total MC variants, while MC-YR increased to represent 45 % of the total MC variants.

3.5. Spatio-temporal distribution of potentially MC-degrading bacteria

The spatio-temporal dynamics of the potentially MC-degrading bacteria were monitored along the freshwater-marine continuum during the pre-bloom, bloom and post-bloom periods (Table S4). The *mlrA* gene was detected in all sampling stations and at all times, but remained mainly below the limit of quantification (< 97.5 copies) and never exceeded 35 *mlrA* gene copies mL^{-1}.

3.6. Intracellular osmolytes concentration

Different intracellular metabolites were investigated and quantified in the cyanobacterial biomass along the freshwater-marine continuum during pre-bloom, bloom and post-bloom periods (Fig. 3C and D). These compounds are categorized as compatible solutes or osmolytes,

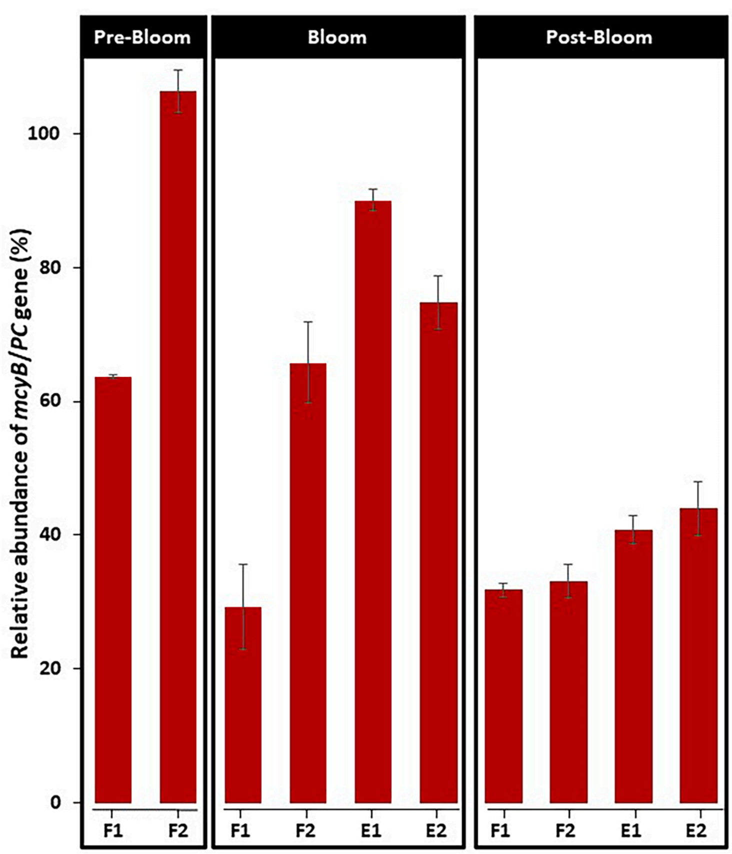

Fig. 2. Dynamics of the relative abundance (%) of *mcyB* gene over the total *Microcystis* population (*PC* gene) along the freshwater-marine continuum (F1, F2, E1, E2) during pre-bloom, bloom and post-bloom campaigns. .

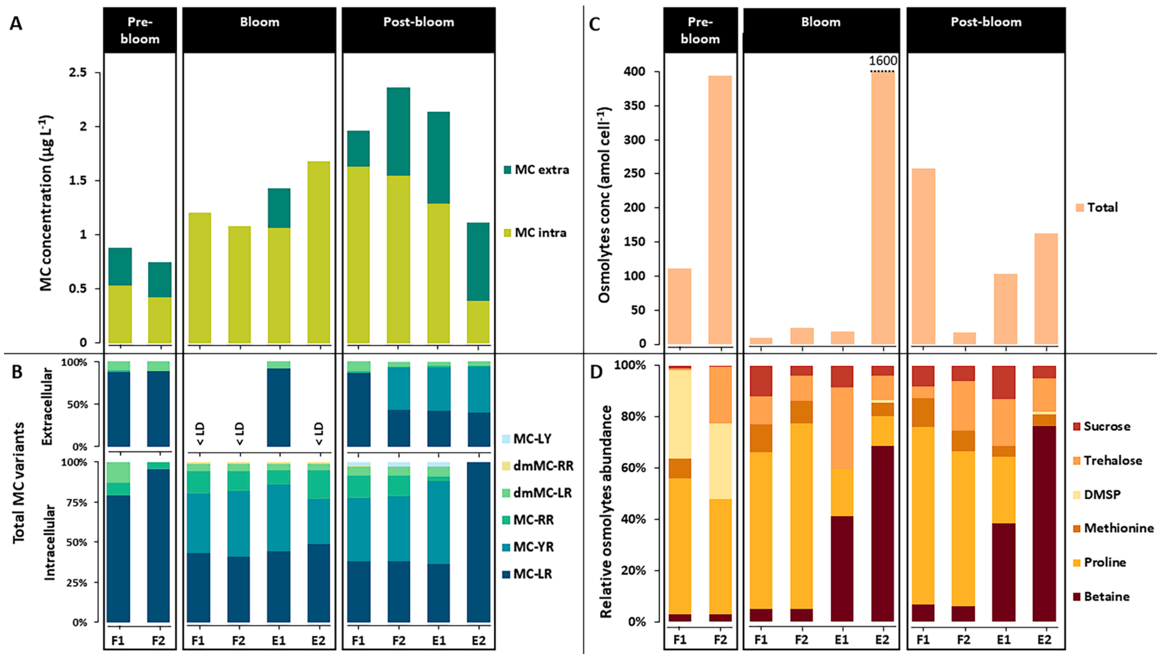

Fig. 3. Dynamic of microcystins and osmolytes along the freshwater-marine continuum (F1, F2, E1, E2) during pre-bloom, bloom and post-bloom campaigns. (**A**) Intracellular and extracellular MC concentrations, (**B**) relative abundance of MC variants expressed as percentage, (**C**) intracellular osmolytes concentration, (**D**) relative abundance of targeted osmolytes expressed as percentage.

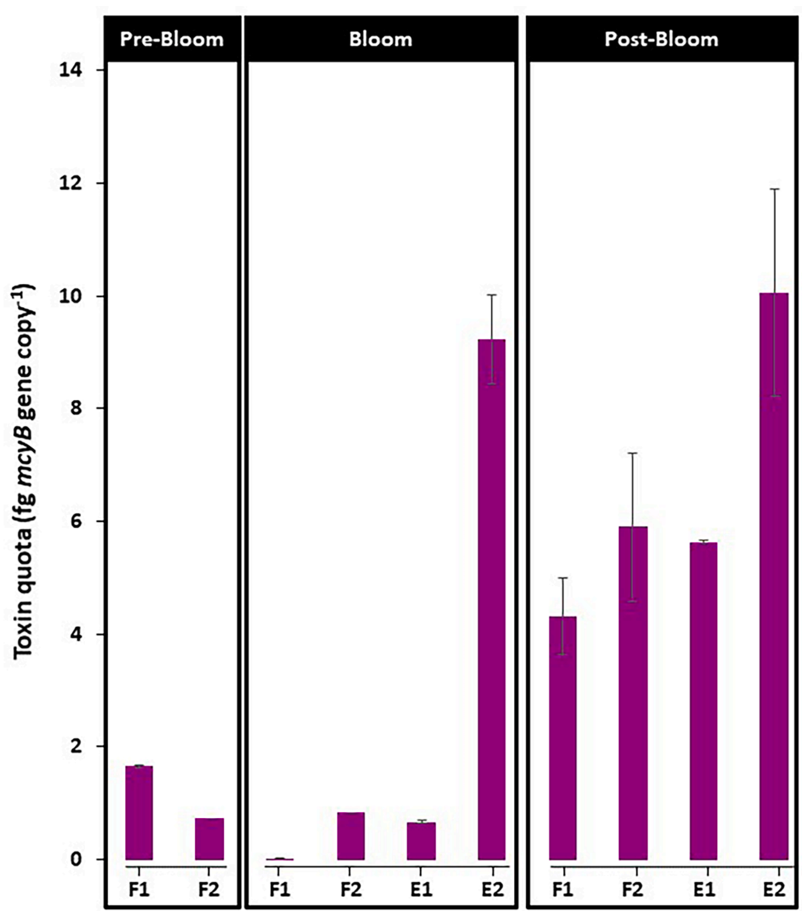

Fig. 4. Dynamic of the toxin quota along the freshwater-marine continuum (F1, F2, E1, E2) during pre-bloom, bloom and post-bloom campaigns.

belonging to the amino acid's family (*i.e.* betaine, proline and methionine), organosulfur compound (DMSP), as well as disaccharides such as sucrose and trehalose.

Total osmolytes concentration increased 175-fold from the freshwater section to the estuarine section during the bloom, with a minimum concentration of 9 amol cell^{-1} at F1 to a maximum of 1.6 × 10^{3} amol cell^{-1} at E2 (Fig. 3C). During the post-bloom, total osmolytes concentration increased 35-fold in the freshwater reservoir (F1) while decreased by 10-fold in the estuary (E2) compared with the bloom period. All six targeted osmolytes were detected in the samples, with the exception of DMSP, which was only detected in freshwater samples during the pre-bloom period (Fig. 3D). During the bloom and post-bloom, the osmolyte profile differed between the freshwater and estuarine sections, with proline being the dominant osmolyte in the freshwater section and betaine in the estuarine section. Along the freshwater-marine continuum more betaine accumulation was observed at the expense of the proline, increasing its concentration more than 2000-fold during bloom (4.5 × 10^{-1} amol cell^{-1} in F1 to 2.0 × 10^{3} amol cell^{-1} in E2) and 7-fold during post-bloom (1.7 × 10^{1} amol cell^{-1} in F1 to 1.2 × 10^{2} amol cell^{-1} in E2). Similarly, among the targeted disaccharides, the freshwater-marine continuum stimulated more trehalose storage by increasing its concentration more than 150-fold during the bloom (9.6 × 10^{-1} amol cell^{-1} at F1 to 1.5 × 10^{2} amol cell^{-1} at E2) and 2-fold during the post-bloom (1.2 × 10^{1} amol cell^{-1} at F1 to 2.1 × 10^{1} amol cell^{-1} at E2). The other two compatible solutes, sucrose and methionine, had similar relative abundances (<10 %).

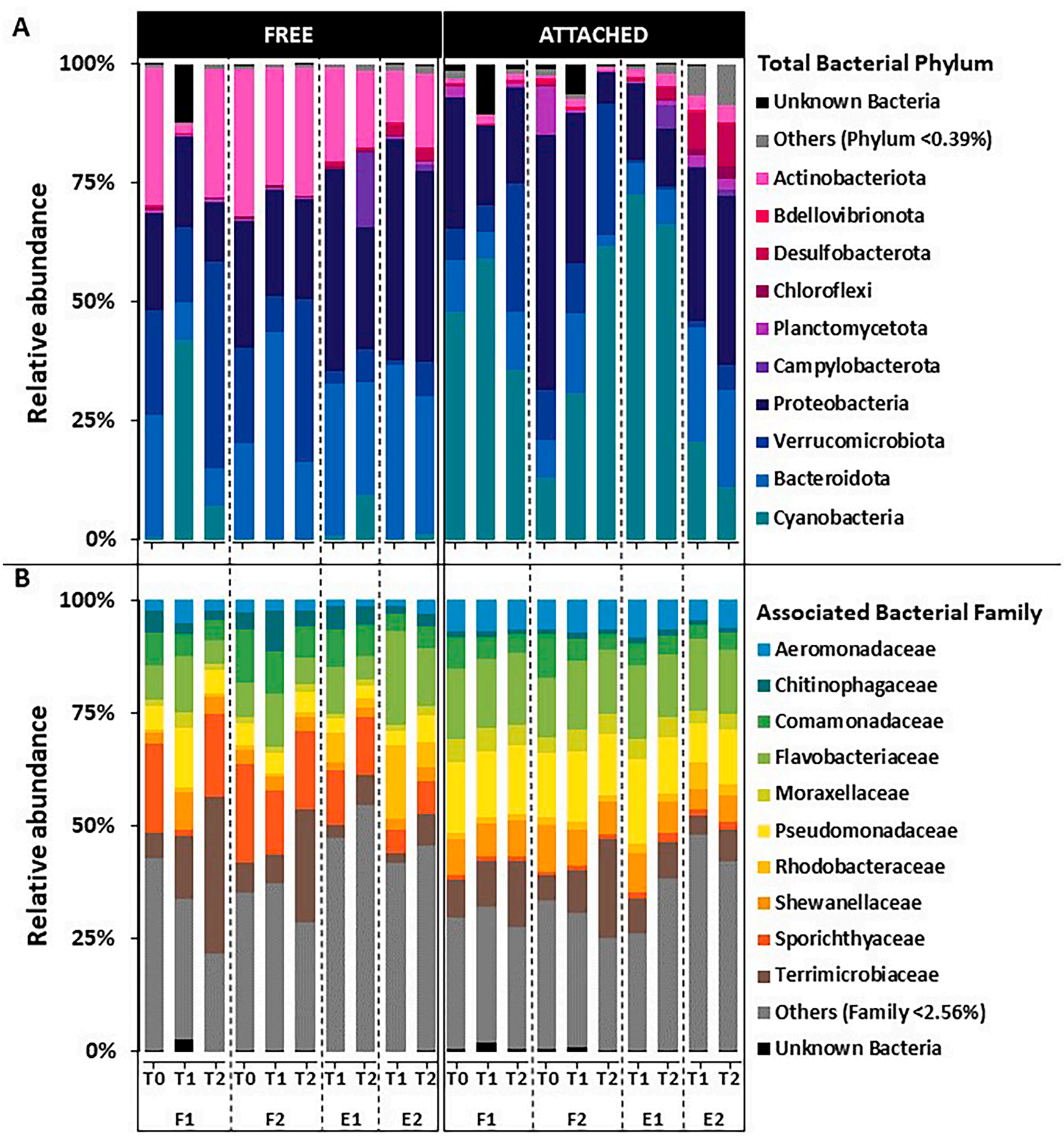

Fig. 5. (**A**) Relative abundances of total bacterial sequences at the phylum level in the free-living (FREE) and attached (ATTACHED) fractions along the freshwater-marine continuum (F1, F2, E1, E2) during pre-bloom (T0), bloom (T1) and post-bloom (T2) campaigns. Phylum less than 0.39 % of the total relative abundance were grouped together as a single group denoted "Others (Phylum < 0.39 %)". **(B)** Relative abundances of the heterotrophic bacterial sequences at the family level. Family less than 2.56 % of the total relative abundance were grouped together as a single group denoted "Others (Family < 2.56 %)".

3.7. Structure and composition of the bacterial community

A total of 1055,100 sequences, matching to 2529 different ASVs, were recovered after quality filtering. After removal of Eukaryota, chloroplasts, mitochondrial and unassigned taxa reads, 1025,233 high-quality reads remained and clustered into 2393 bacterial ASVs. Across samples, most ASVs were assigned to Cyanobacteria (90 ASVs accounting for 27 % of the total reads), Proteobacteria (34 %), Bacteroidota (19 %), Verrucomicrobiota (9 %) and Actinobacteriota (7 %) (Fig. 5A).

The relative abundance of Cyanobacteria ranged from 10 % to 48 % with the highest relative abundances found in the attached fraction (Fig. 5A). The cyanobacterial community was dominated by two families, Microcystaceae and Nostocaceae (Fig. S1). Microcystaceae family was mainly represented by two *Microcystis* ASVs (dae8d and 9314f) accounting for 45 and 23 % of the cyanobacterial community respectively (Fig. S1). Nostocaceae family was mainly represented by one *Dolichospermum* ASV (35,895) accounting for 28 % of the cyanobacterial community (Fig. S1).

Sequences corresponding to Cyanobacteria were removed from the ASV table in order to obtain the heterotrophic bacterial community. As a result, 754,533 reads clustered into 2303 ASVs. Sixty-one percent of the reads were sequenced in the free-living fraction (460,575 reads) and 39 % in the attached fraction (293,958 reads). Richness (Observed and Chao 1) and alpha diversity (Shannon and Pielou) indices of the heterotrophic bacterial community increased along the freshwater-marine continuum, with significantly higher values in the estuarine section (E2) than the two freshwater sites for each fraction (see p-value in

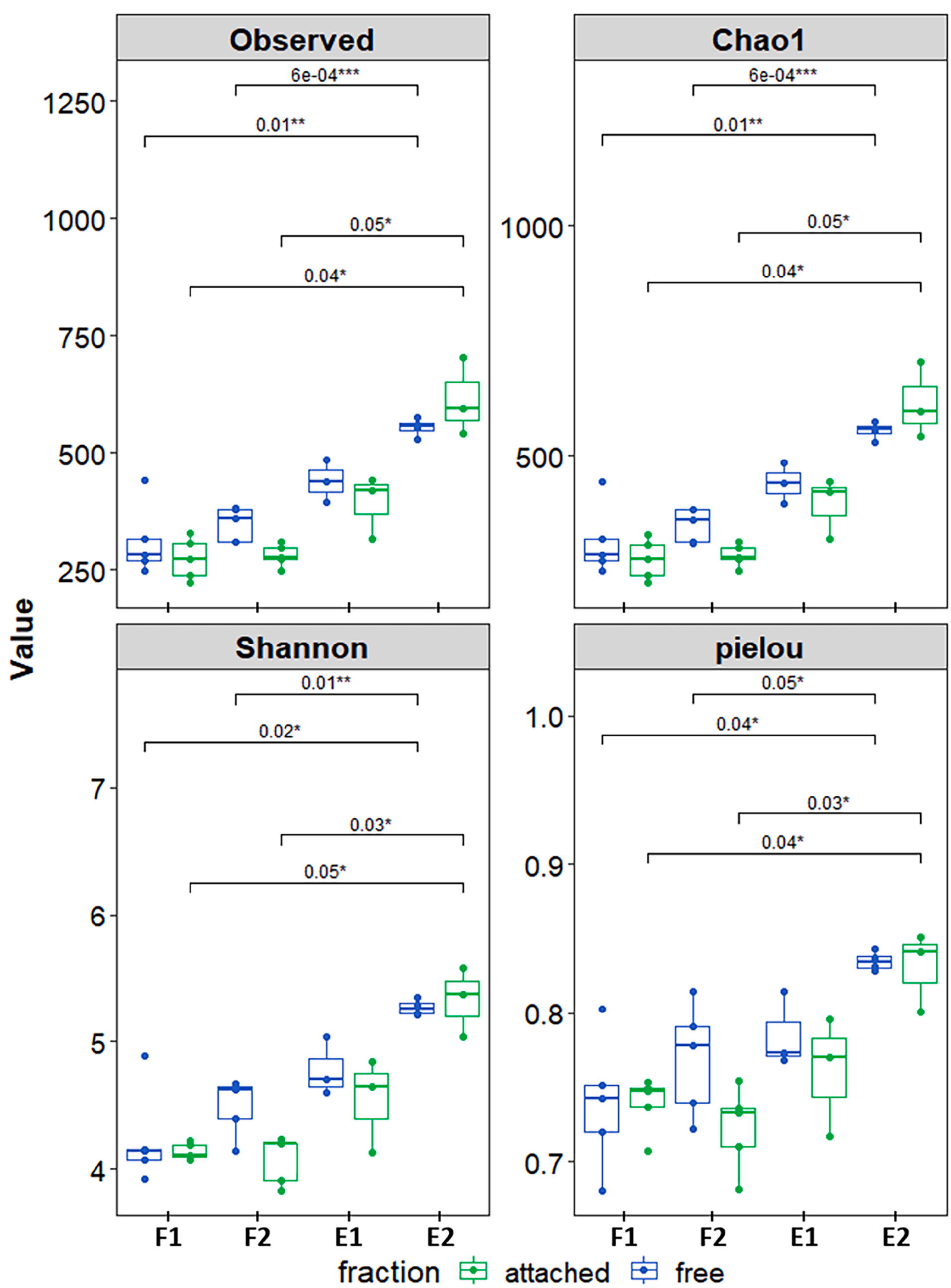

Fig. 6. Alpha diversity box-plot displaying the number of ASVs observed, Chao1, Shannon and Pielou diversity indices for the free-living (in blue) and attached (in green) heterotrophic bacterial communities along the freshwater-marine continuum (F1, F2, E1, E2). Solid lines and asterisks indicate a significant difference between the freshwater section (F1 and F2) and the estuarine section (E1 and E2). P-values were calculated to compare alpha diversities based on a two-sample *t*-test using a non-parametric method with Benjamini-Hochberg correction method.

Fig. 6). No significant difference was observed between the two fractions for each sampling site. Among the top ten families (Fig. 5B), representing 63 % of the heterotrophic bacterial community, families belonging to Gammaproteobacteria (*i.e*. Aeromonadaceae, Comamonadaceae, Moraxellaceae, Pseudomonadaceae, and Shewanellaceae) were dominant in the attached community (7, 5, 4, 14, 8 %, respectively), while Actinobacteria (mostly represented by Sporichthyaceae) and Gammaproteobacteria dominated the free-living community (13 and 19.5 %, respectively).

To investigate dissimilarities between bacterial communities, we performed a non-metric multidimensional scaling (nMDS) analysis based on Bray–Curtis distance metric (Fig. 7). Station, fraction and bloom stage were all significant structuring factors of the bacterial communities with a stress value of 0.0636. More specifically, dissimilarities in the bacterial community composition increased along the freshwater-marine continuum (PERMANOVA R^2 = 34.59, p-value = 0.001) for both distinct attached and free fractions (PERMANOVA R^2 = 22.52, p-value = 0.001), and regardless of bloom stage (PERMANOVA R^2 = 8.81, p-value = 0.003).

We further applied a Linear discriminant analysis Effect Size (LEfSe) on the heterotrophic bacteria dataset. Twenty-four ASVs were identified as biomarkers most likely explaining the differences between heterotrophic bacterial communities along the freshwater-marine continuum (Table S5). They accounted for 49 % of the total heterotrophic bacterial reads. A hierarchical clustering of significant discriminant ASVs was performed and result was visualized in a heatmap (Fig. 8). It clearly showed a clustering of discriminant ASVs according to fraction (free-living and attached) along the freshwater-marine continuum during the bloom.

In the free-living bacterial communities, ASVs belonging to the clusters 2 and 3 were significantly more abundant, while clusters 1 and 4 characterized the attached bacterial communities (except *Terrimicrobium* and *Pseudarcobacter*). Within free-living bacterial communities, the freshwater section differed mainly from the estuarine one by the presence of sequences from *Terrimicrobium, Candidatus Limnoluna, Candidatus Planktophila*, hgcl_clade (8811c and 5320d), *Sporichthyaceae, Sedimicrobacterium* and *Limnohabitans*, while *Pseudarcobacter, Pseudarciella, Fluviicola, Marinobacterium, Unknown Verrumicrobiae* and *Planktomarina* were discriminants ASVs for the estuarine section. Interestingly, in the attached fraction, *Aeromonas, Pseudomonas* (2ad91, b73de and b8ff5), *Shewanella* (f8c9c and 99b11), *FukuN18_freshwater_group, Flavobacterium, Roseomonas* and *Chryseobacterium* were predominantly abundant in the freshwater section, and progressively decreased along the estuary.

To assess whether the mucilage-associated microbiome was conserved along the continuum, we examined the ASVs present in the attached fraction and recovered across all sites, bloom periods and replicates and are defined as core microbiome. Based on the UpSetR analysis, a total of 250 ASVs (257,557 reads) were identified (Table S6). This core microbiome represented 34 % of the total heterotrophic bacterial community. Within the attached bacterial community, the relative abundance of this core microbiome varied from 96 % in the freshwater reservoir (F1) and gradually decreased to 66 % in the estuary (E2) (Table S6). Among the core ASVs members, 15 dominant genera (relative abundance > 1 %) were identified and conserved along the continuum (Fig. 9), such as *Acinetobacter, Aeromonas, Chryseobacterium, Flavobacterium, FukuN18_freshwater_group, Pseudomonas, Roseomonas, Shewanella* and *Terrimicrobium*. Simultaneously, specific microbiomes (Fig. 9) were identified at each station regardless of the bloom stages: 101 ASVs at F1,132 ASVs at F2, 157 ASV at E1 and 578 ASVs at E2, which represented less than 0.4 % of the total reads in the freshwater section (0.2 % at F1, 0.4 % at F2) to 1.4 % at E1 and 6.4 % at E2.

4. Discussion

In this study, we investigated the dynamics of the cyanobacterial population and its associated microbiome along a freshwater-marine continuum. Our objectives were to determine (i) whether increasing salinity induced changes in composition and metabolism of the cyanobacterial community, and (ii) to what extent these changes affected the associated microbiome. We had hypothesized that (1) *Microcystis aeruginosa* would be the most salt tolerant species, (2) that the proportion of potentially toxic species and toxic quotas would increase with the salinity gradient, (3) that an increase in compatible solutes would occur along the continuum as a response to the osmotic stress and (4) that the microbiome associated with the mucilage would be better conserved than in the free fraction. All of our hypotheses were verified to various extent.

4.1. *Cyanobacterial community composition along the freshwater-marine continuum*

During our study *M. aeruginosa* was the dominating species of the freshwater phytoplankton community in the Pen Mur reservoir together with *M. wesenbergii* during the bloom and with *M. wesenbergii* and *Dolichospermum* during the post-bloom. These cyanobacterial species were observed with decreasing cell concentrations along the salinity gradient. These microscopic observations were in agreement with data obtained by 16S rRNA sequencing showing that *Microcystis* and *Dolichospermum* ASVs represented 67 and 28 % respectively of the cyanobacterial community during the study period along the freshwater-marine continuum. The short residence time (of the order of one to two days as estimated in Bormans et al., 2019) would not permit in situ growth of these cyanobacteria. Therefore, we suggest that the decrease in cyanobacterial biomass observed along the continuum can be attributed to the dilution effect of freshwater discharge mixing with estuarine waters even though we minimized that influence by sampling within one hour of low tides. Hence, the salinity gradient was the key factor structuring the

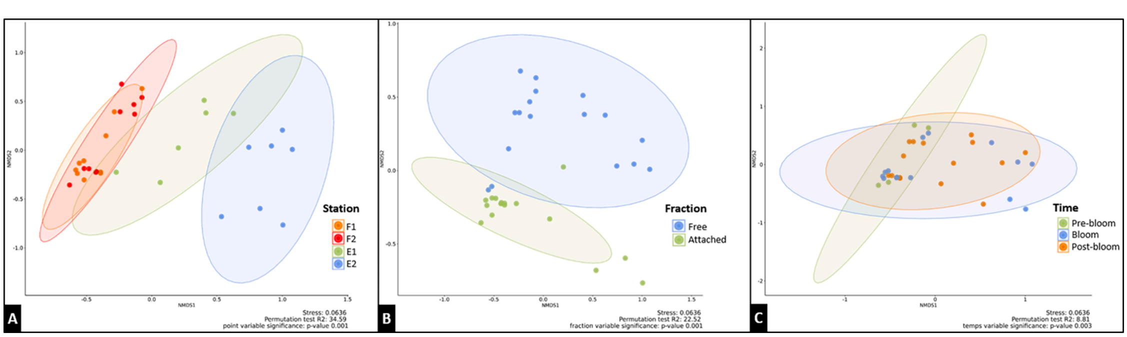

Fig. 7. Non-metric multidimensional scaling (NMDS) ordination, based on Bray–Curtis dissimilarity, of heterotrophic bacterial communities. The plot axes show NMDS scores. Points in the ordination are coloured by hierarchical clustering assignment. The groups were clustered according to (**A**) the freshwater-marine continuum (F1, F2, E1 and E2), (**B**) the fraction (free-living and attached) and (**C**) the bloom stage (Pre-bloom, Bloom and Post-bloom).

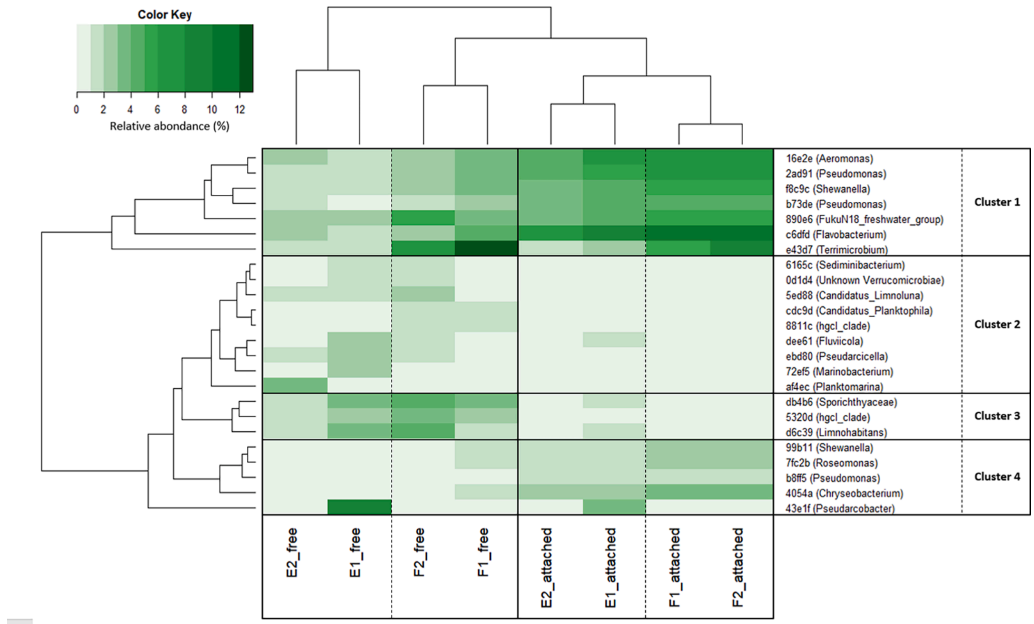

Fig. 8. Heatmap of the hierarchical clustering of significant discriminant ASVs, based of the application of Linear discriminant analysis Effect Size (LEfSe) on the heterotrophic bacteria dataset at the bloom and post-bloom periods. For each ASVs, genus/family/class-level taxonomic assignments are listed.

cyanobacterial community along the studied freshwater-marine continuum.

The Pen Mur freshwater reservoir experiences recurrent *Microcystis* blooms during summer and early autumn which are discharged downstream along a strong gradient of environmental conditions (Bormans et al., 2019, 2020). Nitrate concentration decreased from upstream to downstream suggesting an important freshwater discharge, while phosphate values showed the opposing trend due to sediment resuspension in the estuarine section (Bormans et al., 2019, 2020). Several studies worldwide reported on the cyanobacterial transfer being dominated by *M. aeruginosa* (Preece et al., 2017 for a review), demonstrating a relatively high salinity threshold tolerance of that species, from 4 (Chen et al., 2015) to 18 ppt (Lehman et al., 2005; Lewitus et al., 2008; Tonk et al., 2007). However, our study demonstrated for the first time that other cyanobacterial species, in addition to the well-studied *M. aeruginosa*, have been transferred along a freshwater-marine continuum: *i.e.* either *M. aeruginosa* with *M. botrys* (during the bloom period), or *M. aeruginosa* with *M. botrys, M. wesenbergii* and *Dolichospermum* (during the post-bloom period). Of note, our morphological identifications of the estuary samples (E1, E2) may be impaired as *M. aeruginosa* and *M. botrys* can be confused due to similar colony morphology (Johansson et al., 2019), distinction made even more complex due to salinity-induced changes in colony morphology (*e.g.* cell and colony size; Bormans et al., 2023). Concerning the diazotrophic *Dolichospermum* genus, its occurrence simultaneously with, or alternatively to, *Microcystis* blooms is frequently observed in eutrophic lakes and reservoirs during summer (Cook et al., 2004; Louati et al., 2023; Wang et al., 2013). Notably, *Dolichospermum* spp were noted previously in the Pen Mur reservoir, but so far never in the water column along the continuum, although some akinetes were recorded at F2 in the surface sediments (Bormans et al., 2020). *Dolichospermum* can also withstand high salinities of up to 15 g L^{-1} NaCl in their natural brackish environment (*i.e.* the Baltic Sea, Moisander et al. 2002) and up to 24 g L^{-1} NaCl in salt stress experiments (Houliez et al., 2021), which may explain their maintenance in estuarine sites during our study. Finally, although *M. wesenbergii* has received less attention due to its potential non-toxicity characteristic (Xu et al., 2008), it is also distributed in the freshwater environments widely around the world, notably in Asia (Son et al., 2005), Europe (Jasprica et al., 2005), America (Oberholster et al., 2006) and Oceania (Wood et al., 2005). Recently, we have shown that *M. wesenbergii* is at least as salt-tolerant as the well-studied *M. aeruginosa*, notably due to its thick mucilage layer (Reignier et al., 2023). Further physiological studies on this species would be of interest to better understand its capacity to cope under salinity stress condition.

Overall, the cyanobacterial community, dominated by a *Microcystis* spp. assemblage, was transferred across the freshwater-marine continuum. In the following, we will attempt to explain the mechanisms involved in the response to salt stress of this *Microcystis* community.

4.2. Insight into salt tolerance of Microcystis spp

The mechanisms of salinity tolerance in *Microcystis* are still unclear and could be related to inter- and intraspecific tolerances to salt exposure (Preece et al., 2017). While the mucilage associated with the colonial form of *Microcystis* can be seen as one external defense strategy against salinity (Bormans et al., 2023; Kruk et al., 2017; Reignier et al., 2023), the compatible solutes accumulation is one of the main internal defense strategies identified in the literature (Georges des Aulnois et al., 2019; Hagemann, 2011). In our study, the total compatible solutes concentration targeted increased 175-fold from the freshwater section to the estuarine section during the bloom. Wang et al. (2022) also found a significant increase in various compatible solutes like sucrose or methionine in natural colonies of *Microcystis* in saline water simulation experiment ($S = 5$ and $S = 10$).

Pade and Hagemann (2015) considered that this internal defense strategy in cyanobacteria occurred primarily *via* the production and accumulation of small organic molecules (osmolytes) to increase internal osmolarity, ensure water uptake and maintain cells turgescence. The internal defense against salinity can also occur *via* the active transport of compatible solutes from the environment. For instance, *Aphanothece halophytica* demonstrates uptake systems for glycine betaine (Moore et al., 1987), whereas *Synechocystis* has been found to have uptake systems for sucrose and trehalose (Mikkat et al., 1997). While trehalose and sucrose are mainly produced by freshwater strains, betaine and possibly proline dominate in halophilic strains and the major compatible solutes usually correlate with the salinity tolerance (Pade and Hagemann, 2015). In this study, trehalose accumulation/storage increased (150-fold) along the freshwater-marine continuum during

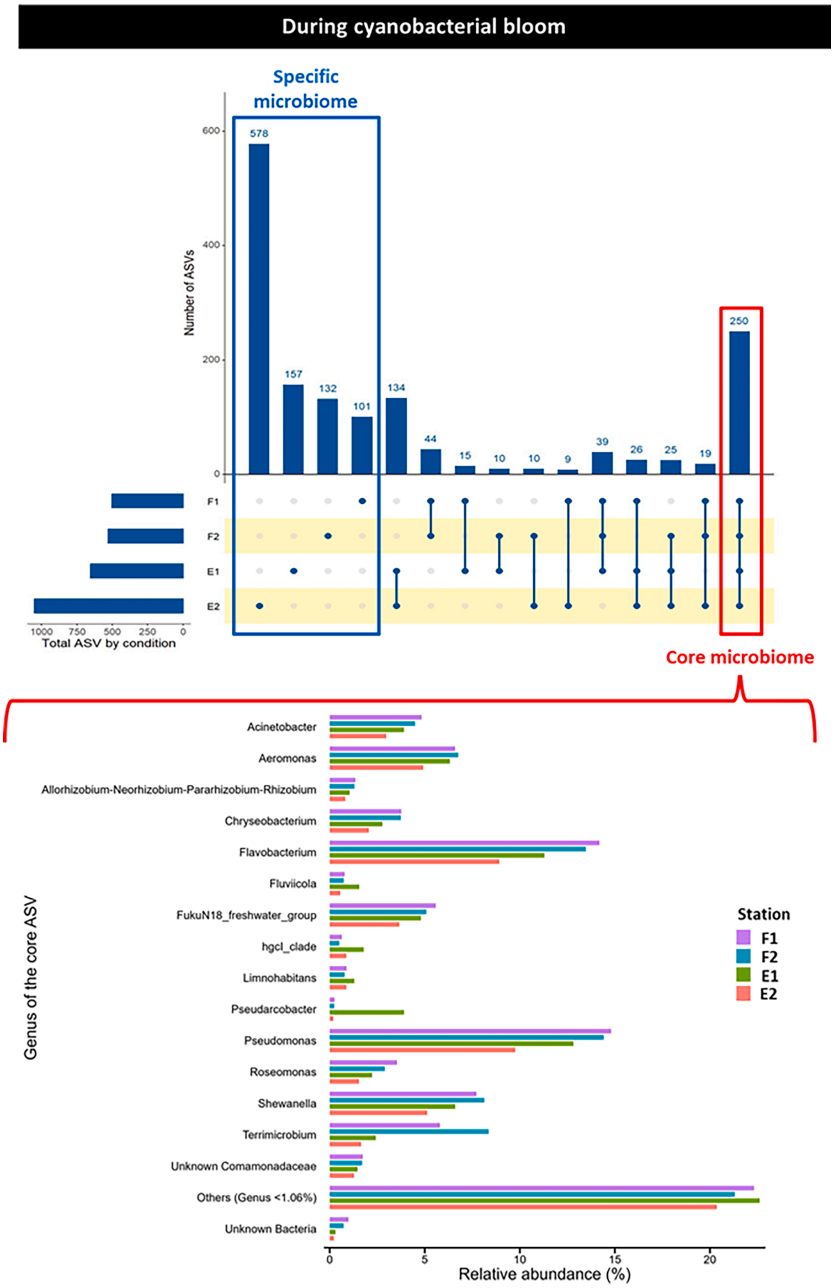

Fig. 9. UpSetR plot showing the number of specific or shared ASVs within the attached fraction in each sampling sites. The bars show the overlap between the indicated samples below. The bottom panel shows the relative abundances of the main ASVs shared between the four sampling sites.

cyanobacterial bloom. This observation confirms a halotolerance response of freshwater *Microcystis* colonies along the salinity gradient, as trehalose is mainly produced by freshwater *Microcystis* strains (Georges des Aulnois et al., 2019; Hagemann, 2011). Sucrose did not increase along the continuum supporting the view that sucrose is produced particularly by highly halotolerant brackish cyanobacterial strains (Georges des Aulnois et al., 2020; Kolman et al., 2012; Tanabe et al., 2018). In this study, betaine accumulation increased (2000-fold) along the freshwater-marine continuum during cyanobacterial bloom, compared to proline or methionine. Betaine improves water availability (Gabbay-Azaria et al., 1988; Sadak and Ahmed, 2016) and protects growth and photosynthesis enzymes (Sakamoto and Murata, 2002), while proline, acting as a secondary osmoprotector (Waditee-Sirisattha et al., 2022), is known to regulate oxidative stress induced by salt stress (Kishor et al., 1995), and cellular pH (Bellinger, 1987). Betaine was found to act as a compatible solute for *M. aeruginosa* strains acclimatised to increasing salinities (Georges des Aulnois et al., 2019). Nevertheless, betaine is best known as the main osmoprotector in the most salt-tolerant groups of marine cyanobacteria (Kageyama and Waditee-Sirisattha, 2022) and also found in a wide range of other bacteria and plants, so we cannot rule out the hypothesis that betaine came from species more halotolerant than *Microcystis*. Finally, DMSP was only detected in freshwater samples during the pre-bloom period. Described as a putative compatible solute in marine algae (Stefels, 2000), rarely detected in cyanobacteria (Oren, 2007) and not detected in *M. aeruginosa* strains (Georges des Aulnois et al., 2019), we suggest that DMSP was originating from diatoms, chlorophytes or even halophytic plants present in the Pen Mur freshwater reservoir and known to be rich sources of DMSP (Kageyama and Waditee-Sirisattha, 2022).

4.3. Transfer of the potential toxicity along the freshwater-marine continuum

In our study, whereas the *Microcystis* biomass decreased along the freshwater-continuum, the relative abundance of potentially MC-producing *Microcystis* increased along the freshwater-marine continuum. To our knowledge, this is the first study to report the selection of potentially MC-producing *Microcystis* within a *Microcystis* community along a salinity gradient. Several studies reported spatio-temporal dynamics of relative abundance of potentially MC-producing strains within *Microcystis* blooms in freshwater ecosystems, and very different results can be found from lake to lake and from a single lake over time (Briand et al., 2009; Kurmayer and Kutzenberger, 2003; Lezcano et al., 2018; Sabart et al., 2010). What emerges from these studies is the importance of the effect of local environmental conditions on the fitness of potentially MC-producing and non-MC-producing subpopulations. Only one study has looked at the spatio-temporal dynamics of toxic *Microcystis* genotypes along a salinity gradient, the 800 km continuum of the Rio Uruguay de la Plata (Martínez de la Escalera et al., 2017), but without relating it to the abundance of the total *Microcystis* population. Hence, whereas the authors observed a decreased in toxic *Microcystis* genotypes along the continuum, likely due to a dilution effect, their results highlighted the capacity to toxic genotypes to tolerate high-salinity conditions, which is consistent with our observations. However, we acknowledge that considering only one of the ten *mcy* genes to estimate the relative abundance of toxic *Microcystis* genotypes is not sufficient to cover all possible genetic variability and to confidently assess genotype selection according to environmental conditions.

In the present study, despite relatively low MCs concentrations (up to 60 times lower than those found in 2017 in the freshwater section according to Bormans et al. (2019)), the intracellular MCs content of toxic genotypes notably increased along the freshwater-marine continuum. Hence, the *mcyB* genotypes in the estuary were up to 2- to 500-fold more toxic than those in the freshwater reservoir during the post-bloom and the bloom, respectively. Diverse environmental, nutritional, and biological conditions can modulate MCs synthesis (see for reviews Boopathi and Ki, 2014; Liu et al., 2022; Neilan et al., 2013). Concerning the influence of salinity on MCs production, studies carried out to date, exclusively experimental and on single-cell strains of *Microcystis*, have found no impact on MCs production and suggest that MCs quotas do not respond to salt stress (Georges Des Aulnois et al., 2019, 2020; Tanabe et al., 2018 and references herein). Nevertheless, salt shock induces oxidative stress (Ross et al., 2019) and MCs have been found to protect cells from oxidative stress by binding and stabilizing proteins (Zilliges et al., 2011). This raises the question of whether such a mechanism can occur in natural *Microcystis* colonies along the continuum and would participate in the better capacity to tolerate salt shock by MC-producing *Microcystis* cells.

Here, we observed higher concentrations of extracellular MC downstream, likely due to cyanobacterial cell lyses at elevated salinity (Tonk et al., 2007) and the dominance of three highly toxic variants (*i.e.* MC-LR, MC-YR, and dmMC-LR). These dominant MCs variants were transferred without specific selection along the salinity gradient, as already mentioned in a previous study of this continuum (Bormans et al., 2019). Overall, these results are worrying and reinforce the need for continuous evaluation of risk exposure to MCs in this location as it can impact/contaminate estuarine even marine organisms (Amzil et al., 2023; Ger et al., 2018; Gupta et al., 2003; Lance et al., 2010; Lehman et al., 2008; Otten et al., 2017).

The relatively low level of toxicity measured in this study could be the result of many factors, including dilution, adsorption, abiotic or biotic degradation. MCs released into the environment are chemically stable and do not degrade easily, even following changes in light intensity, pH and temperature (Harada et al., 1996; Tsuji et al., 1995, 1996). For these reasons, the main degradation pathway for MCs is essentially biological, particularly bacterial (Bourne et al., 2006). The *mlr* pathway is currently the main known mechanism for MCs biodegradation and involves four specialized enzymes encoded by *mlrABCD* genes (Bourne et al., 1996, 2001). However, MC-degrading genotypes bacteria with *mlrA* gene were not abundant during our study and not selected along the freshwater-marine continuum. Consistently, very few taxa belonging to the Sphingomonadacea family (*i.e. Sphingomonas, Sphyngopyxis* and *Novosphingobium*) and reported to possess *mlr* genes and to degrade MCs (Massey and Yang, 2020) were found in our sequencing dataset (<0.2 % of the total reads of the heterotroph bacterial community). Nevertheless, the absence of *mlr* genes in some isolated MC-degrading bacteria (Thees et al., 2019; Lezcano et al., 2016; Manage, 2009), along with the relationships observed between *mlr*-lacking bacteria able to degrade organic complex compounds and toxic cyanobacterial blooms (Kraufeldt et al., 2019; Lezcano et al., 2017; Mou et al., 2013), support the hypothesis that there are bacteria lacking *mlr* genes involved in the degradation of MCs in the environment. This suggests the existence of alternative-*mlr* MC degradation pathways operating in nature, which may involve glutathione S-transferases and alkaline proteases (as indicated by Kraufeldt et al., 2019; Mou et al., 2013; Takenaka and Watanabe, 1997). More studies would be required to explore this hypothesis.

4.4. Heterotrophic bacterial community associated with Microcystis spp. and its transfer along the continuum

The dominant bacterial phyla recovered in all samples (*i.e.* Proteobacteria, Bacteroidetes, Actinobacteria, and Verrucomicrobia), were phyla frequently observed in association with freshwater cyanobacterial blooms (Li et al., 2020; Te et al., 2023; Tromas et al., 2017). These phyla are also prevalent in aquatic environments characterized by dynamic salinity shifts due to tidal action and variable freshwater inputs, as observed along short hydrological retention times (Herlemann et al., 2011; Murray et al., 1996). At the ASVs level, our findings reveal significant alterations in the composition and structure of the bacterial community. Spatial factors emerge as the primary influence, followed by the fraction and bloom period, underscoring the significance of salinity in shaping the microbiome structure along the freshwater-marine continuum. Shifts in bacterial community composition along aquatic salinity gradients have been documented in several studies (Cottrell and David, 2003; Crump et al., 1999; Herlemann et al., 2011; Kan et al., 2008; Kirchman et al., 2005; Murray et al., 1996). Here, the richness and diversity of the heterotrophic bacterial community increased along the freshwater-marine continuum. Similar trend was observed along a short (5 km) continuum in New Zealand (Tee et al., 2021). The authors suggested that the greater diversity observed in marine water compared to freshwater in short continuum may be attributed to ASVs being flushed out to the estuary. This hypothesis is supported by our findings showing that over 55 % of ASVs were shared between stations. Contrasting results can be found in the literature, with studies that showed no clear trend (Herlemann et al., 2011, 2016) or a reduction in diversity with increasing salinity along longer continuum (more than 2000 km long) (Doherty et al., 2017; Mason et al., 2016).

In accordance with the literature, the free-living and attached bacterial community were distinct and differed mainly by the abundance of Actinobacteria (mostly represented by Sporichthyaceae) which was much higher in the free-living bacterial community in all samples (10–20 % of the sequences) compared to less than 5 % in the attached fraction. In previous studies on the composition of the free-living bacterial community from various French lakes, Actinobacteria accounted for 20–60 % of the sequences (Boucher et al., 2006; Debroas et al., 2009; Humbert et al., 2009; Parveen et al., 2013), and similar findings were obtained in other countries (*e.g.* Sekar et al., 2003; Shi et al., 2012; Warnecke et al., 2004). While Actinobacteria are more abundant in pelagic freshwater habitats (Allgaier and Grossart, 2006; Glöckner et al., 2000; Sekar et al., 2003; Warnecke et al., 2005) than pelagic marine environments (Pommier et al., 2007), they remain significant members of the autochthonous estuarine community (*e.g.* in the central Baltic Sea proper (Riemann et al., 2008) or in the Delaware Estuary (Kirchman et al., 2005), displaying adaptability to estuarine gradients (Kirchman et al., 2005; Langenheder et al., 2003; Stevens et al., 2007).

Previous studies on phytoplankton aggregates dominated by *Microcystis* have suggested that the *Microcystis* phycosphere hosts a distinct bacterial community compared to free-living communities, characterized by enrichment in Alpha, Gamma-proteobacteria and Bacteroidia and depletion in Actinobacteria (Jankowiak and Gobler, 2020; Louati et al., 2015; Parveen et al., 2013; Zhu et al., 2019). Specifically, we identified ten ASVs affiliated to either Gammaproteobacteria (*Aeromonas, Pseudomonas* 2ad91, b73de and b8ff5, *Shewanella* f8c9c and 99b11), or Alphaproteobacteria (*Roseomonas*), Bacteroidia (*Flavobacterium* and *Chryseobacterium*) and Verrucomicrobiae (*FukuN18_freshwater_group*), being biomarkers of the freshwater attached bacterial community. These taxa are commonly associated with cyanobacterial blooms, notably those of *Microcystis* (Crevecoeur et al., 2023; Eiler and Bertilsson, 2004; Jankowiak and Gobler, 2020; Kim et al., 2020; Parveen et al., 2013; Zheng et al., 2020), suggesting their potential adaptation to cyanobacteria-induced conditions and their role in degrading cyanobacteria-derived dissolved organic matter. Interestingly, these biomarkers also constitute major members of the core microbiome (attached bacteria conserved along the continuum), demonstrating a high degree of connectivity along the freshwater-marine continuum, despite a strong environmental gradient. The question of whether these taxa are retrieved along the salinity gradient because they are still embedded in the mucus of *Microcystis* or attached to particulate organic matter remains unresolved and requires further investigation. Nevertheless, it is tempting to suggest that these bacteria, prevalent in the fraction associated with *Microcystis* in the freshwater section, may still be embedded in the mucus of *Microcystis* along the continuum, forming the *Microcystis* core microbiome. Within the mucilaginous colony, bacteria and *Microcystis* cells find a favorable environment to thrive, being physically protected against the salinity gradient and situated in a nutrient-rich habitat. One of the keys to the success of *Microcystis* in changing environments could be the cooperative microbial network. Previous studies have revealed close functional complementation between *Microcystis* and attached bacteria (Li et al., 2018), some involving taxa found in the *Microcystis* core microbiome of our study. Examples include metabolic interdependencies between *Microcystis* and *Roseomonas* for carotenoid synthesis (Pérez-Carrascal et al., 2021), between *M. aeruginosa* and attached *Pseudomonas* sp. in the phosphorus cycle (Jiang et al., 2007), and the capability of both *Flavobacterium* and Verrucomicrobiae to degrade cyanobacteria-derived complex organic compounds (Berg et al., 2009; Betiku et al., 2021). While some bacteria facilitate the growth of cyanobacteria, others can prevent them from developing. Potentially algicidal bacteria, such as *Chryseobacterium* and *Shewanella* (Li et al., 2014; Zhang et al., 2019), were identified in the *Microcystis* core microbiome. Additionally, potentially pathogenic bacteria like *Aeromonas* and *Pseudomonas* (Berg et al., 2009), known to cause adverse health effects in humans and animals, were also present and should be considered when assessing the risks associated with cyanobacterial blooms and their transfer.

5. Conclusions

In conclusion, the study provides a better understanding of the dynamics of cyanobacterial communities, particularly dominated by *Microcystis* spp., along a freshwater-marine continuum in the Pen Mur reservoir. Within this gradient, *M. aeruginosa* stands out as the most halotolerant, followed by *M. wesenbergii*, which benefits from a thick mucilage layer providing physical protection against osmotic shock. Additionally, trehalose, betaine, and other osmoprotectors play essential roles in facilitating adaptation to diverse salinity levels. These findings illuminate the internal defense strategies employed by these cyanobacteria to thrive in environments characterized by varying salinities.

Our research highlights the transfer of potentially toxic *Microcystis* genotypes across the continuum, with an increase in intracellular MC concentrations downstream, emphasizing the need for continuous monitoring due to potential ecological and health risks.

Furthermore, the study delves into the heterotrophic bacterial community associated with *Microcystis*, revealing a highly conserved mucilage-associated microbiome along the continuum. The findings underline the crucial need to characterize the interactions that take place within natural *Microcystis* colonies with its microbiome, and to determine their impact on *Microcystis*' fitness and ability to adapt to various environmental conditions, which could be the key to their widespread success worldwide (Cook et al., 2020; Pound et al., 2021).

CRediT authorship contribution statement

Océane Reignier: Writing – original draft, Visualization, Investigation, Formal analysis. **Myriam Bormans:** Writing – review & editing, Validation, Supervision, Conceptualization. **Fabienne Hervé:** Writing – review & editing, Methodology, Investigation. **Elise Robert:** Writing – review & editing, Methodology, Investigation. **Véronique Savar:** Writing – review & editing, Methodology, Investigation. **Simon Tanniou:** Writing – review & editing, Methodology, Investigation. **Zouher Amzil:** Writing – review & editing, Supervision. **Cyril Noël:** Writing – review & editing, Software, Resources. **Enora Briand:** Writing – review & editing, Validation, Supervision, Funding acquisition, Conceptualization.

Declaration of competing interest

The authors declare that they have no known competing financial interests or personal relationships that could have appeared to influence the work reported in this paper.

Data availability

We have shared the links to our sequencing data and R scripts in the main manuscript. The others data will be made available on request.

Acknowledgements

We acknowledge Ifremer for the Ph.D. funding of Océane Reignier. Moreover, we would like to thank Nathalie Le Bris for performing the nutrient analyses at the EcoChim platform of the OSUR (Rennes, France), Dr. Maria Angeles Lezcano (CAB, Madrid, Spain) for kindly providing us the IM-2 strain of *Sphingopyxis* sp., and Ifremer LER-MPL laboratory (Nantes, France) for the loan of physico-chemical probes.

Supplementary materials

Supplementary material associated with this article can be found, in the online version, at doi:10.1016/j.hal.2024.102627.

References

Allgaier, M., Grossart, HP., 2006. Diversity and seasonal dynamics of Actinobacteria populations in four lakes in northeastern Germany. Appl. Environ. Microbiol. 72 (5), 3489–3497.
Aminot, A., & Chaussepied, M. (1983). *Manuel des analyses chimiques en milieu marin.*
Aminot, A., & Kérouel, R. (2004). *Hydrologie des écosystèmes marins: paramètres et analyses.* Editions Quae.
Amzil, Z., Derrien, A., Terre Terrillon, A., Savar, V., Bertin, T., Peyrat, M., Duval, A., Lhaute, K., Arnich, N., Hort, V., Nicolas, M., 2023. Five years monitoring the emergence of unregulated toxins in shellfish in France (EMERGTOX 2018-2022). Mar. Drugs 21 (8), 435.
Bashir, F., Bashir, A., Bouaïcha, N., Chen, L., Codd, G.A., Neilan, B., Xu, WL., Ziko, L., Rajput, V.D., Minkina, T., 2023. Cyanotoxins, biosynthetic gene clusters, and factors modulating cyanotoxin biosynthesis. World J. Microbiol. Biotechnol. 39 (9), 241.

Bell, W., Mitchell, R., 1972. Chemotactic and growth responses of marine bacteria to algal extracellular products. Biol. Bull. 143 (2), 265–277.

Bellinger, Y., 1987. Proline accumulation in higher plants: a redox buffer? Plant Physiol. (Life Sci. Adv.) 6, 23–27.

Berg, K.a, Lyra, C., Sivonen, K., Paulin, L., Suomalainen, S., Tuomi, P., Rapala, J., 2009. High diversity of cultivable heterotrophic bacteria in association with cyanobacterial water blooms. ISMe J. 3 (3), 314–325.

Betiku, O.C., Sarjeant, K.C., Ngatia, L.W., Aghimien, M.O., Odewumi, C.O., Latinwo, L. M., 2021. Evaluation of microbial diversity of three recreational water bodies using 16S rRNA metagenomic approach. Sci. Total Environ. 771, 144773.

Black, K., Yilmaz, M., Phlips, E.J., 2011. Growth and toxin production by *Microcystis Aeruginosa* PCC 7806 (Kutzing) lemmerman at elevated salt concentrations. J. Environ. Prot. (Irvine,. Calif) 02 (06), 669–674.

Bolyen, E., Rideout, J.R., Dillon, M.R., Bokulich, N.A., Abnet, C.C., Al-Ghalith, G.A., Alexander, H., Alm, E.J., Arumugam, M., Asnicar, F., 2019. Reproducible, interactive, scalable and extensible microbiome data science using QIIME 2. Nat. Biotechnol. 37 (8), 852–857.

Bonnet, M.P., Poulin, M., 2002. Numerical modelling of the planktonic succession in a nutrient-rich reservoir: environmental and physiological factors leading to *Microcystis aeruginosa* dominance. Ecol. Modell. 156 (2–3), 93–112.

Boopathi, T., Ki, JS., 2014. Impact of environmental factors on the regulation of cyanotoxin production. Toxins. (Basel) 6 (7), 1951–1978.

Bormans, M., Amzil, Z., Mineaud, E., Brient, L., Savar, V., Robert, E., Lance, E., 2019. Demonstrated transfer of cyanobacteria and cyanotoxins along a freshwater-marine continuum in France. Harmful. Algae 87, 101639.

Bormans, M., Legrand, B., Waisbord, N., Briand, E., 2023. Morphological and Physiological Impacts of Salinity on Colonial Strains of the Cyanobacteria *Microcystis aeruginosa*, 12. MicrobiologyOpen, pp. 1–10.

Bormans, M., Savar, V., Legrand, B., Mineaud, E., Robert, E., Lance, E., Amzil, Z., 2020. Cyanobacteria and cyanotoxins in estuarine water and sediment. Aquat. Ecol. 54, 625–640.

Boucher, D., Jardillier, L., Debroas, D., 2006. Succession of bacterial community composition over two consecutive years in two aquatic systems: a natural lake and a lake-reservoir. FEMS Microbiol. Ecol. 55 (1), 79–97.

Bourelly, P., 1985. Les Algues d'eau douce: initiation à la systématique. Tome III: Les Algues Bleues Et Rouge. Boubee, Paris.

Bourne, D.G., Blakeley, R.L., Riddles, P., Jones, G.J., 2006. Biodegradation of the cyanobacterial toxin microcystin LR in natural water and biologically active slow sand filters. Water Res. 40 (6), 1294–1302.

Bourne, D.G., Jones, G.J., Blakeley, R.L., Jones, A., Negri, A.P., Riddles, P., 1996. Enzymatic pathway for the bacterial degradation of the cyanobacterial cyclic peptide toxin microcystin LR. Appl. Environ. Microbiol. 62 (11), 4086–4094.

Bourne, D.G., Riddles, P., Jones, G.J., Smith, W., Blakeley, R.L., 2001. Characterisation of a gene cluster involved in bacterial degradation of the cyanobacterial toxin microcystin LR. Environ. Toxicol. 16 (6), 523–534.

Briand, E., Bormans, M., Gugger, M., Dorrestein, P.C., Gerwick, W.H., 2016. Changes in secondary metabolic profiles of *Microcystis aeruginosa* strains in response to intraspecific interactions. Environ. Microbiol. 18 (2), 384–400.

Briand, E., Escoffier, N., Straub, C., Sabart, M., Quiblier, C., Humbert, JF., 2009. Spatiotemporal changes in the genetic diversity of a bloom-forming *Microcystis aeruginosa* (cyanobacteria) population. ISMe J. 3 (4), 419–429.

Bukaveckas, P.A., Lesutienė, J., Gasiūnaitė, Z.R., Ložys, L., Olenina, I., Pilkaitytė, R., Pūtys, Ž., Tassone, S., Wood, J., 2017. Microcystin in aquatic food webs of the Baltic and Chesapeake Bay regions. Estuar. Coast. Shelf. Sci. 191, 50–59.

Callahan, B.J., McMurdie, P.J., Rosen, M.J., Han, A.W., Johnson, A.J.A., Holmes, S.P., 2016. DADA2: high-resolution sample inference from Illumina amplicon data. Nat. Methods 13 (7), 581–583.

Casamatta, D.A., Wickstrom, C.E., 2000. Sensitivity of two disjunct bacterioplankton communities to exudates from the cyanobacterium *Microcystis aeruginosa* Kützing. Microb. Ecol. 40 (1), 64–73.

Chen, L., Mao, F., Kirumba, G.C., Jiang, C., Manefield, M., He, Y., 2015. Changes in metabolites, antioxidant system, and gene expression in *Microcystis aeruginosa* under sodium chloride stress. Ecotoxicol. Environ. Saf. 122, 126–135.

Conway, J.R., Lex, A., Gehlenborg, N., 2017. UpSetR: an R package for the visualization of intersecting sets and their properties. Bioinformatics 33 (18), 2938–2940.

Cook, C.M., Vardaka, E., Lanaras, T., 2004. Toxic cyanobacteria in Greek freshwaters, 1987—2000: occurrence, toxicity, and impacts in the mediterranean region. Acta Hydrochim. Hydrobiol. 32 (2), 107–124.

Cook, K.V., Li, C., Cai, H., Krumholz, L.R., Hambright, K.D., Paerl, H.W., Steffen, M.M., Wilson, A.E., Burford, M.A., Grossart, H., 2020. The global *Microcystis* interactome. Limnol. Oceanogr. 65, S194–S207.

Costanza, R., De Groot, R., Sutton, P., Van der Ploeg, S., Anderson, S.J., Kubiszewski, I., Farber, S., Turner, R.K., 2014. Changes in the global value of ecosystem services. Glob. Environ. Change 26, 152–158.

Cottrell, M.T., David, K.L., 2003. Contribution of major bacterial groups to bacterial biomass production (thymidine and leucine incorporation) in the Delaware estuary. Limnol. Oceanogr. 48 (1), 168–178.

Crevecoeur, S., Edge, T.A., Watson, L.C., Watson, S.B., Greer, C.W., Ciborowski, J.J.H., Diep, N., Dove, A., Drouillard, K.G., Frenken, T., 2023. Spatio-temporal connectivity of the aquatic microbiome associated with cyanobacterial blooms along a Great Lake riverine-lacustrine continuum. Front. Microbiol. 14, 1073753.

Crump, B.C., Armbrust, E.V., Baross, J.A., 1999. Phylogenetic analysis of particle-attached and free-living bacterial communities in the Columbia River, its estuary, and the adjacent coastal ocean. Appl. Environ. Microbiol. 65 (7), 3192–3204.

Curson, A.R.J., Williams, B.T., Pinchbeck, B.J., Sims, L.P., Martínez, A.B., Rivera, P.P.L., Kumaresan, D., Mercadé, E., Spurgin, L.G., Carrión, O., 2018. DSYB catalyses the key step of dimethylsulfoniopropionate biosynthesis in many phytoplankton. Nat. Microbiol. 3 (4), 430–439.

de Souza, M.S., Muelbert, J.H., Costa, L.D.F., Klering, E.V., Yunes, J.S., 2018. Environmental variability and cyanobacterial blooms in a subtropical coastal lagoon: searching for a sign of climate change effects. Front. Microbiol. 9, 1727.

Debroas, D., Humbert, JF., Enault, F., Bronner, G., Faubladier, M., Cornillot, E., 2009. Metagenomic approach studying the taxonomic and functional diversity of the bacterial community in a mesotrophic lake (Lac du Bourget - France). Environ. Microbiol. 11 (9), 2412–2424.

Di Tommaso, P., Chatzou, M., Floden, E.W., Barja, P.P., Palumbo, E., Notredame, C., 2017. Nextflow enables reproducible computational workflows. Nat. Biotechnol. 35 (4), 316–319.

Doherty, M., Yager, P.L., Moran, M.A., Coles, V.J., Fortunato, C.S., Krusche, A.V., Medeiros, P.M., Payet, J.P., Richey, J.E., Satinsky, B.M., 2017. Bacterial biogeography across the Amazon River-ocean continuum. Front. Microbiol. 8, 882.

Eiler, A., Bertilsson, S., 2004. Composition of freshwater bacterial communities associated with cyanobacterial blooms in four Swedish lakes. Environ. Microbiol. 6 (12), 1228–1243.

Eiler, A., Olsson, J.A., Bertilsson, S., 2006. Diurnal variations in the auto- and heterotrophic activity of cyanobacterial phycospheres (*Gloeotrichia echinulata*) and the identity of attached bacteria. Freshw. Biol. 51 (2), 298–311.

Erratt, K.J., Creed, I.F., Lobb, D.A., Smol, J.P., Trick, C.G., 2023. Climate change amplifies the risk of potentially toxigenic cyanobacteria. Glob. Chang. Biol. 29 (18), 5240–5249.

Fuks, D., Radić, J., Radić, T., Najdek, M., Blažina, M., Degobbis, D., Smodlaka, N., 2005. Relationships between heterotrophic bacteria and cyanobacteria in the northern Adriatic in relation to the mucilage phenomenon. Sci. Total Environ. 353 (1–3), 178–188.

Fulton, R.S., Paerl, H.W., 1987. Toxic and inhibitory effects of the blue-green alga *Microcystis aeruginosa* on herbivorous zooplankton. J. Plankton Res. 9 (5), 837–855.

Gabbay-Azaria, R., Tel-Or, E., Schönfeld, M., 1988. Glycinebetaine as an osmoregulant and compatible solute in the marine cyanobacterium *Spirulina subsalsa*. Arch. Biochem. Biophys. 264 (1), 333–339.

Georges des Aulnois, M., Réveillon, D., Robert, E., Caruana, A., Briand, E., Guljamow, A., Dittmann, E., Amzil, Z., Bormans, M., 2020. Salt shock responses of *Microcystis* revealed through physiological, transcript, and metabolomic analyses. Toxins. (Basel) 12 (3), 192–210.

Georges des Aulnois, M., Roux, P., Caruana, A., Réveillon, D., Briand, E., Hervé, F., Savar, V., Bormans, M., Amzil, Z., 2019. Physiological and metabolic responses of freshwater and brackish-water strains of *Microcystis aeruginosa* acclimated to a salinity gradient: insight into salt tolerance. Appl. Environ. Microbiol. 85 (21), e01614–19.

Ger, K.A., Otten, T.G., DuMais, R., Ignoffo, T., Kimmerer, W., 2018. *In situ* ingestion of *Microcystis* is negatively related to copepod abundance in the upper San Francisco Estuary. Limnol. Oceanogr. 63 (6), 2394–2410.

Gibble, C.M., Peacock, M.B., Kudela, R.M., 2016. Evidence of freshwater algal toxins in marine shellfish: implications for human and aquatic health. Harmful. Algae 59, 59–66.

Glöckner, F.O., Yilmaz, P., Quast, C., Gerken, J., Beccati, A., Ciuprina, A., Bruns, G., Yarza, P., Peplies, J., Westram, R., Ludwig, W., 2017. 25 years of serving the community with ribosomal RNA gene reference databases and tools. J. Biotechnol. 261, 169–176.

Glöckner, F.O., Zaichikov, E., Belkova, N., Denissova, L., Pernthaler, J., Pernthaler, A., Amann, R., 2000. Comparative 16S rRNA analysis of lake bacterioplankton reveals globally distributed phylogenetic clusters including an abundant group of actinobacteria. Appl. Environ. Microbiol. 66 (11), 5053–5065.

Gupta, N., Pant, S.C., Vijayaraghavan, R., Rao, P.V.L., 2003. Comparative toxicity evaluation of cyanobacterial cyclic peptide toxin microcystin variants (LR, RR, YR) in mice. Toxicology 188 (2–3), 285–296.

Hagemann, M., 2011. Molecular biology of cyanobacterial salt acclimation. FEMS Microbiol. Rev. 35 (1), 87–123.

Harada, K., Tsuji, K., Watanabe, M.F., Kondo, F., 1996. Stability of microcystins from cyanobacteria—III. Effect of pH and temperature. Phycologia 35 (sup6), 83–88.

Henriksen, A., Selmer-Olsen, A.R., 1970. Automatic methods for determining nitrate and nitrite in water and soil extracts. Analyst 95 (1130), 514–518.

Herlemann, D.P.R., Labrenz, M., Jürgens, K., Bertilsson, S., Waniek, J.J., Andersson, A.F., 2011. Transitions in bacterial communities along the 2000km salinity gradient of the Baltic Sea. ISME J. 5 (10), 1571–1579.

Herlemann, D.P.R., Lundin, D., Andersson, A.F., Labrenz, M., Jürgens, K., 2016. Phylogenetic signals of salinity and season in bacterial community composition across the salinity gradient of the Baltic Sea. Front. Microbiol. 7, 1883.

Houliez, E., Briand, E., Malo, F., Rovillon, G.A., Hervé, F., Robert, E., Marchand, L., Zykwinska, A., Caruana, A.M.N., 2021. Physiological changes induced by sodium chloride stress in *Aphanizomenon gracile, Cylindrospermopsis raciborskii* and *Dolichospermum* sp. Harmful. Algae 103, 102028.

Humbert, JF., Dorigo, U., Cecchi, P., Le Berre, B., Debroas, D., Bouvy, M., 2009. Comparison of the structure and composition of bacterial communities from temperate and tropical freshwater ecosystems. Environ. Microbiol. 11 (9), 2339–2350.

ISO, B.S., 1999. 8245. *Water Quality—Guidelines for the Determination of Total Organic Carbon (TOC) and Dissolved Organic Carbon (DOC)*. British Standard Institution, London.

ISO, I., 2005. Standard 20179: 2005. Water quality–Determination of Microcystins–Method Using Solid Phase Extraction (SPE) and High Performance Liquid Chromatography (HPLC) With Ultraviolet (UV) Detection. International Organization for Standardization, Geneva.

Jackrel, S.L., Yang, J.W., Schmidt, K.C., Denef, V.J., 2021. Host specificity of microbiome assembly and its fitness effects in phytoplankton. ISMe J. 15 (3), 774–788.
Jankowiak, J.G., & Gobler, C.J. (2020). The composition and function of microbiomes within *Microcystis* colonies are significantly different than native bacterial assemblages in two North American Lakes. 11, 1016.
Jasprica, N., Hafner, D., Batistić, M., Kapetanović, T., 2005. Phytoplankton in three freshwater lakes in the Neretva River delta (Eastern Adriatic, NE Mediterranean). Nova Hedwigia. 81 (1–2), 37–54.
Jiang, L., Yang, L., Xiao, L., Shi, X., Gao, G., Qin, B., 2007. Quantitative studies on phosphorus transference occuring between *Microcystis aeruginosa* and its attached bacterium (*Pseudomonas* sp.). Hydrobiologia 581 (1), 161–165.
Johansson, E., Legrand, C., Björnerås, C., Godhe, A., Mazur-Marzec, H., Säll, T., Rengefors, K., 2019. High diversity of microcystin chemotypes within a summer bloom of the cyanobacterium *Microcystis botrys*. Toxins. (Basel) 11 (12), 1–16.
Kaebernick, M., Neilan, B.A., 2001. Ecological and molecular investigations of cyanotoxin production. FEMS Microbiol. Ecol. 35 (1), 1–9.
Kageyama, H., Waditee-Sirisattha, R., 2022. Chapter 9 - Osmoprotectant Molecules in Cyanobacteria: Their Basic Features, Biosynthetic Regulations, and Potential Applications. Academic Press, pp. 113–123. H. Kageyama & R. B. TC. P. Waditee-Sirisattha (eds.).
Kan, J., Evans, S.E., Chen, F., Suzuki, M.T., 2008. Novel estuarine bacterioplankton in rRNA operon libraries from the Chesapeake Bay. Aquat. Microbial Ecol. 51 (1), 55–66.
Kehr, J.C., Dittmann, E., 2015. Biosynthesis and function of extracellular glycans in cyanobacteria. Life 5 (1), 164–180.
Kim, M., Lee, J., Yang, D., Park, H.Y., Park, W., 2020. Seasonal dynamics of the bacterial communities associated with cyanobacterial blooms in the Han River. Environ. Pollut. 266, 115198.
Kirchman, D.L., Dittel, A.I., Malmstrom, R.R., Cottrell, M.T., 2005. Biogeography of major bacterial groups in the Delaware Estuary. Limnol. Oceanogr. 50 (5), 1697–1706.
Kishor, P.B.K., Hong, Z., Miao, GH., Hu, CA.A., Verma, D.P.S., 1995. Overexpression of [delta]-pyrroline-5-carboxylate synthetase increases proline production and confers osmotolerance in transgenic plants. Plant Physiol. 108 (4), 1387–1394.
Kolman, M.A., Torres, L.L., Martin, M.L., Salerno, G.L., 2012. Sucrose synthase in unicellular cyanobacteria and its relationship with salt and hypoxic stress. Planta 235 (5), 955–964.
Komárek, J., & Anagnostidis, K.C. (2008). Teil 1/Part 1: Chroococcales. *Süßwasserflora Von Mitteleuropa;* Ettl,H., Gerloff,J., Heynig,H., Mollenhauer,D.*, Eds*, 1–556.
Krausfeldt, L.E., Steffen, M., McKay, R.M., Bullerjahn, G.S., Boyer, G.L., Wilhelm, S.W., 2019. Insight into the molecular mechanisms for microcystin biodegradation in Lake Erie and Lake Taihu. Front. Microbiol. 10, 2741.
Kruk, C., Segura, A.M., Nogueira, L., Alcántara, I., Calliari, D., Martínez de la Escalera, G., Carballo, C., Cabrera, C., Sarthou, F., Scavone, P., Piccini, C., 2017. A multilevel trait-based approach to the ecological performance of *Microcystis aeruginosa* complex from headwaters to the ocean. Harmful. Algae 70, 23–36.
Kurmayer, R., Kutzenberger, T., 2003. Application of real-time PCR for quantification of microcystin genotypes in a population of the toxic cyanobacterium *Microcystis* sp. Appl. Environ. Microbiol. 69 (11), 6723–6730.
Lance, E., Brient, L., Carpentier, A., Acou, A., Marion, L., Bormans, M., Gérard, C., 2010. Impact of toxic cyanobacteria on gastropods and microcystin accumulation in a eutrophic lake (Grand-Lieu, France) with special reference to *Physa* (= *Physella*) *acuta*. Sci. Total Environ. 408 (17), 3560–3568.
Lance, E., Lepoutre, A., Savar, V., Robert, E., Bormans, M., Amzil, Z., 2021. *In situ* use of bivalves and passive samplers to reveal water contamination by microcystins along a freshwater-marine continuum in France. Water Res. 204, 117620.
Langenheder, S., Kisand, V., Wikner, J., Tranvik, L.J., 2003. Salinity as a structuring factor for the composition and performance of bacterioplankton degrading riverine DOC. FEMS Microbiol. Ecol. 45 (2), 189–202.
Laplace-Treyture, C., Barbe, J., Dutartre, A., Druart, J.C., Rimet, F., & Anneville, O. (2009). *Standard protocol for Sampling, Conservation, Observation and Counting of Lake Phytoplankton for application of the WFD: version 3.3. 1*.
Lehman, P.W., Boyer, G., Hall, C., Waller, S., Gehrts, K., 2005. Distribution and toxicity of a new colonial *Microcystis aeruginosa* bloom in the San Francisco Bay Estuary, California. Hydrobiologia 541, 87–99.
Lehman, P.W., Boyer, G., Satchwell, M., Waller, S., 2008. The influence of environmental conditions on the seasonal variation of *Microcystis* cell density and microcystins concentration in San Francisco Estuary. Hydrobiologia 600 (1), 187–204.
Lewitus, A.J., Brock, L.M., Burke, M.K., DeMattio, K.A., Wilde, S.B., 2008. Lagoonal stormwater detention ponds as promoters of harmful algal blooms and eutrophication along the South Carolina coast. Harmful. Algae 8 (1), 60–65.
Lezcano, M.Á., Morón-López, J., Agha, R., López-Heras, I., Nozal, L., Quesada, A., El-Shehawy, R., 2016. Presence or absence of *mlr* genes and nutrient concentrations co-determine the microcystin biodegradation efficiency of a natural bacterial community. Toxins. (Basel) 8 (11), 318.
Lezcano, M.Á., Quesada, A., El-Shehawy, R., 2018. Seasonal dynamics of microcystin-degrading bacteria and toxic cyanobacterial blooms: interaction and influence of abiotic factors. Harmful. Algae 71, 19–28.
Lezcano, M.Á., Velázquez, D., Quesada, A., El-Shehawy, R., 2017. Diversity and temporal shifts of the bacterial community associated with a toxic cyanobacterial bloom: an interplay between microcystin producers and degraders. Water Res. 125, 52–61.
Li, H., Barber, M., Lu, J., Goel, R., 2020. Microbial community successions and their dynamic functions during harmful cyanobacterial blooms in a freshwater lake. Water Res. 185, 116292.
Li, Z., Lin, S., Liu, X., Tan, J., Pan, J., Yang, H., 2014. A freshwater bacterial strain, *Shewanella* sp. Lzh-2, isolated from Lake Taihu and its two algicidal active substances, hexahydropyrrolo [1, 2-a] pyrazine-1, 4-dione and 2, 3-indolinedione. Appl. Microbiol. Biotechnol. 98, 4737–4748.
Li, Q., Lin, F., Yang, C., Wang, J., Lin, Y., Shen, M., Park, M.S., Li, T., Zhao, J., 2018. A large-scale comparative metagenomic study reveals the functional interactions in six bloom-forming Microcystis-epibiont communities. Front. Microbiol. 9, 746.
Liu, J., Chen, L., Zhang, X., 2022. Current research scenario for biological effect of exogenous factors on microcystin synthesis. Environ. Sci. Pollut. Res. 29 (18), 26190–26201.
Louati, I., Nunan, N., Tambosco, K., Bernard, C., Humbert, JF., Leloup, J., 2023. The phyto-bacterioplankton couple in a shallow freshwater ecosystem: who leads the dance? Harmful. Algae 126, 102436.
Louati, I., Pascault, N., Debroas, D., Bernard, C., Humbert, JF., Leloup, J., 2015. Structural Diversity of Bacterial Communities Associated with Bloom-Forming Freshwater Cyanobacteria Differs According to the Cyanobacterial Genus. PLoS. One 10 (11), e0140614.
Lozupone, C., Knight, R., 2005. UniFrac: a new phylogenetic method for comparing microbial communities. Appl. Environ. Microbiol. 71 (12), 8228–8235.
Manage, P.M., 2009. Seasonal changes in the abundance of biological agents killing *Microcystis aeruginosa* in a hypereutrophic pond. Vidyodaya J. Sci. 14, 85–101.
Martin, M., 2011. Cutadapt removes adapter sequences from high-throughput sequencing reads. EMBnet. J. 17 (1), 10–12.
Martínez de la Escalera, G., Kruk, C., Segura, A.M., Nogueira, L., Alcántara, I., Piccini, C., 2017. Dynamics of toxic genotypes of *Microcystis aeruginosa* complex (MAC) through a wide freshwater to marine environmental gradient. Harmful. Algae 62, 73–83.
Mason, O.U., Canter, E.J., Gillies, L.E., Paisie, T.K., Roberts, B.J., 2016. Mississippi River plume enriches microbial diversity in the Northern Gulf of Mexico. Front. Microbiol. 7, 1048.
Massey, I.Y., Yang, F., 2020. A mini review on microcystins and bacterial degradation. Toxins. (Basel) 12 (4), 268.
Mikalsen, B., Boison, G., Skulberg, O.M., Fastner, J., Davies, W., Gabrielsen, T.M., Rudi, K., Jakobsen, K.S., 2003. Natural variation in the microcystin synthetase operon *mcyABC* and impact on microcystin production in *Microcystis* strains. J. Bacteriol. 185 (9), 2774–2785.
Mikkat, S., Effmert, U., Hagemann, M., 1997. Uptake and use of the osmoprotective compounds trehalose, glucosylglycerol, and sucrose by the cyanobacterium *Synechocystis* sp. PCC6803. Arch. Microbiol. 167 (2–3), 112–118.
Miller, M.A., Kudela, R.M., Mekebri, A., Crane, D., Oates, S.C., Tinker, M.T., Staedler, M., Miller, W.A., Toy-Choutka, S., Dominik, C., 2010. Evidence for a novel marine harmful algal bloom: cyanotoxin (microcystin) transfer from land to sea otters. PLoS. One 5 (9), e12576.
Moisander, P.H., McClinton, E., Paerl, H.W., 2002. Salinity effects on growth, photosynthetic parameters, and nitrogenase activity in estuarine planktonic cyanobacteria. Microb. Ecol. 43, 432–442.
Moore, D.J., Reed, R.H., Stewart, W.D.P., 1987. A glycine betaine transport system in *Aphanothece halophytica* and other glycine betaine-synthesising cyanobacteria. Arch. Microbiol. 147, 399–405.
Mou, X., Lu, X., Jacob, J., Sun, S., Heath, R., 2013. Metagenomic identification of bacterioplankton taxa and pathways involved in Microcystin degradation in Lake Erie. PLoS. One 8 (4), e61890.
Murphy, J., Riley, J.P., 1962. A modified single solution method for the determination of phosphate in natural waters. Anal. Chim. Acta 27 (C), 31–36.
Murray, A.E., Hollibaugh, J.T., Orrego, C., 1996. Phylogenetic compositions of bacterioplankton from two California estuaries compared by denaturing gradient gel electrophoresis of 16S rDNA fragments. Appl. Environ. Microbiol. 62 (7), 2676–2680.
Neilan, B.a, Pearson, L.a, Muenchhoff, J., Moffitt, M.C., Dittmann, E., 2013. Environmental conditions that influence toxin biosynthesis in cyanobacteria. Environ. Microbiol. 15 (5), 1239–1253.
Neu, A.T., Allen, E.E., Roy, K., 2021. Defining and quantifying the core microbiome: challenges and prospects. Proc. Natl. Acad. Sci. 118 (51), e2104429118.
O'Neil, J.M., Davis, T.W., Burford, M.A., Gobler, C.J., 2012. The rise of harmful cyanobacteria blooms: the potential roles of eutrophication and climate change. Harmful. Algae 14, 313–334.
Oberholster, P.J., Botha, A., Cloete, T.E., 2006. Toxic cyanobacterial blooms in a shallow, artificially mixed Urban Lake in Colorado, USA. In: Lakes Reservoirs: Res. Manag., 11, pp. 111–123.
Olesen, S.W., Duvallet, C., Alm, E.J., 2017. dbOTU3: a new implementation of distribution-based OTU calling. PLoS. One 12 (5), e0176335.
Oren, A., 2007. Diversity of organic osmotic compounds and osmotic adaptation in cyanobacteria and algae. Algae and Cyanobacteria in Extreme Environments. Springer, pp. 639–655.
Orr, P.T., Jones, G.J., Douglas, G.B., 2004. Response of cultured *Microcystis aeruginosa* from the Swan River, Australia, to elevated salt concentration and consequences for bloom and toxin management in estuaries. Mar. Freshw. Res. 55 (3), 277.
Otten, T.G., Paerl, H.W., Dreher, T.W., Kimmerer, W.J., Parker, A.E., 2017. The molecular ecology of *Microcystis* sp. blooms in the San Francisco Estuary. Environ. Microbiol. 19 (9), 3619–3637.
Ozaki, K., Ohta, A., Iwata, C., Horikawa, A., Tsuji, K., Ito, E., Ikai, Y., Harada, KI., 2008. Lysis of cyanobacteria with volatile organic compounds. Chemosphere 71 (8), 1531–1538.
Pade, N., Hagemann, M., 2015. Salt acclimation of cyanobacteria and their application in biotechnology. Life 5 (1), 25–49.
Paerl, H.W., Otten, T.G., Kudela, R., 2018. Mitigating the expansion of harmful algal blooms across the freshwater-to-marine continuum. Environ. Sci. Technol. 52 (10), 5519–5529.

Parada, A.E., Needham, D.M., Fuhrman, J.A., 2016. Every base matters: assessing small subunit rRNA primers for marine microbiomes with mock communities, time series and global field samples. Environ. Microbiol. 18 (5), 1403–1414.
Parveen, B., Ravet, V., Djediat, C., Mary, I., Quiblier, C., Debroas, D., Humbert, J., 2013. Bacterial communities associated with *Microcystis* colonies differ from free-living communities living in the same ecosystem. Environ. Microbiol. Rep. 5 (5), 716–724.
Peacock, M.B., Gibble, C.M., Senn, D.B., Cloern, J.E., Kudela, R.M., 2018. Blurred lines: multiple freshwater and marine algal toxins at the land-sea interface of San Francisco Bay, California. Harmful. Algae 73, 138–147.
Penn, K., Wang, J., Fernando, S.C., Thompson, J.R., 2014. Secondary metabolite gene expression and interplay of bacterial functions in a tropical freshwater cyanobacterial bloom. ISMe J. 8 (9), 1866–1878.
Pérez-Carrascal, O.M., Tromas, N., Terrat, Y., Moreno, E., Giani, A., Corrêa Braga Marques, L., Fortin, N., Shapiro, B.J., 2021. Single-colony sequencing reveals microbe-by-microbiome phylosymbiosis between the cyanobacterium *Microcystis* and its associated bacteria. Microbiome 9 (1), 194.
Pommier, T., Canbäck, B., Riemann, L., Boström, K.H., Simu, K., Lundberg, P., Tunlid, A., Hagström, Å., 2007. Global patterns of diversity and community structure in marine bacterioplankton. Mol. Ecol. 16 (4), 867–880.
Pound, H.L., Martin, R.M., Sheik, C.S., Steffen, M.M., Newell, S.E., Dick, G.J., McKay, R. M.L., Bullerjahn, G.S., Wilhelm, S.W., 2021. Environmental studies of cyanobacterial harmful algal blooms should include interactions with the dynamic microbiome. Environ. Sci. Technol. 55 (19), 12776–12779.
Preece, E.P., Hardy, F.J., Moore, B.C., Bryan, M., 2017. A review of microcystin detections in Estuarine and Marine waters: environmental implications and human health risk. Harmful. Algae 61, 31–45.
Quast, C., Pruesse, E., Yilmaz, P., Gerken, J., Schweer, T., Yarza, P., Peplies, J., Glöckner, F.O., 2012. The SILVA ribosomal RNA gene database project: improved data processing and web-based tools. Nucleic Acids Res. 41 (D1), D590–D596.
Rainer, K., Thomas, K., 2003. Application of real-time PCR for quantification of microcystin genotypes in a population of the toxic cyanobacterium *Microcystis* sp. Appl. Environ. Microbiol. 69 (11), 6723–6730.
Rashidan, K.K., Bird, D.F., 2001. Role of predatory bacteria in the termination of a cyanobacterial bloom. Microb. Ecol. 41, 97–105.
Reignier, O., Bormans, M., Marchand, L., Sinquin, C., Amzil, Z., Zykwinska, A., Briand, E., 2023. Production and composition of extracellular polymeric substances by a unicellular strain and natural colonies of *Microcystis*: impact of salinity and nutrient stress. Environ. Microbiol. Rep. 15 (6), 783–796.
Réveillon, D., Georges des Aulnois, M., Savar, V., Robert, E., Caruana, A.M.N., Briand, E., Bormans, M., 2024. Extraction and analysis by liquid chromatography – tandem mass spectrometry of intra- and extracellular microcystins and nodularin to study the fate of cyanobacteria and cyanotoxins across the freshwater-marine continuum. Toxicon. 237, 107551.
Reynolds, C.S., 2007. Variability in the provision and function of mucilage in phytoplankton: facultative responses to the environment. Hydrobiologia 578 (1), 37–45.
Riemann, L., Leitet, C., Pommier, T., Simu, K., Holmfeldt, K., Larsson, U., Hagstrom, A., 2008. The native bacterioplankton community in the central Baltic Sea is influenced by freshwater bacterial species. Appl. Environ. Microbiol. 74 (2), 503–515.
Rigosi, A., Carey, C.C., Ibelings, B.W., Brookes, J.D., 2014. The interaction between climate warming and eutrophication to promote cyanobacteria is dependent on trophic state and varies among taxa. Limnol. Oceanogr. 59 (1), 99–114.
Robson, B.J., Hamilton, D.P., 2003. Summer flow event induces a cyanobacterial bloom in a seasonal Western Australian estuary. Mar. Freshw. Res. 54 (2), 139–151.
Ross, C., Warhurst, B.C., Brown, A., Huff, C., Ochrietor, J.D., 2019. Mesohaline conditions represent the threshold for oxidative stress, cell death and toxin release in the cyanobacterium *Microcystis aeruginosa*. Aquat. Toxicol. 206, 203–211.
Sabart, M., Pobel, D., Briand, E., Combourieu, B., Salençon, M.J., Humbert, JF., Latour, D., 2010. Spatiotemporal variations in microcystin concentrations and in the proportions of microcystin-producing cells in several *Microcystis aeruginosa* populations. Appl. Environ. Microbiol. 76 (14), 4750–4759.
Sadak, M.S., Ahmed, M.R.M., 2016. Physiological role of cyanobacteria and glycine betaine on wheat plant grown under salinity stress. Int. J. Pharm Tech Res. 9, 78–92.
Saito, T., Okano, K., Park, HD., Itayama, T., Inamori, Y., Neilan, B.a., Burns, B.P., Sugiura, N., 2003. Detection and sequencing of the microcystin LR-degrading gene, *mlrA*, from new bacteria isolated from Japanese lakes. FEMS Microbiol. Lett. 229 (2), 271–276.
Sakamoto, A., Murata, N., 2002. The role of glycine betaine in the protection of plants from stress: clues from transgenic plants. Plant Cell Environ. 25 (2), 163–171.
Sampognaro, L., Eirín, K., Martínez de la Escalera, G., Piccini, C., Segura, A., Kruk, C., 2020. Experimental evidence on the effects of temperature and salinity in morphological traits of the *Microcystis aeruginosa* complex. J. Microbiol. Methods 175, 105971.
Sandrini, G., Huisman, J., Matthijs, H.C.P., 2015. Potassium sensitivity differs among strains of the harmful cyanobacterium *Microcystis* and correlates with the presence of salt tolerance genes. FEMS Microbiol. Lett. 362 (16), fnv121.
Sekar, R., Pernthaler, A., Pernthaler, J., Warnecke, F., Posch, T., Amann, R., 2003. An improved protocol for quantification of freshwater Actinobacteria by fluorescence in situ hybridization. Appl. Environ. Microbiol. 69 (5), 2928–2935.
Shen, H., Niu, Y., Xie, P., Tao, M., Yang, X., 2011. Morphological and physiological changes in *Microcystis aeruginosa* as a result of interactions with heterotrophic bacteria. Freshw. Biol. 56 (6), 1065–1080.
Shi, L., Cai, Y., Kong, F., Yu, Y., 2012. Specific association between bacteria and buoyant *Microcystis* colonies compared with other bulk bacterial communities in the eutrophic Lake Taihu, China. Environ. Microbiol. Rep. 4 (6), 669–678.
Son, MH., Zulfugarov, I.S., Kwon, O., Moon, BY., Chung, IK., Lee, CH., Lee, J., 2005. The study on the fluorescence characteristics of several freshwater bloom forming algal species and its application. Algae 20 (2), 113–120.
Stefels, J., 2000. Physiological aspects of the production and conversion of DMSP in marine algae and higher plants. J. Sea Res. 43 (3–4), 183–197.
Stevens, H., Brinkhoff, T., Rink, B., Vollmers, J., Simon, M., 2007. Diversity and abundance of Gram positive bacteria in a tidal flat ecosystem. Environ. Microbiol. 9 (7), 1810–1822.
Sun, J., Liu, D., 2003. Geometric models for calculating cell biovolume and surface area for phytoplankton. J. Plankton Res. 25 (11), 1331–1346.
Takenaka, S., Watanabe, M.F., 1997. Microcystin-LR degradation by *Pseudomonas aeruginosa* alkaline protease. Chemosphere 34, 749–757.
Tanabe, Y., Hodoki, Y., Sano, T., Tada, K., Watanabe, M.M., 2018. Adaptation of the freshwater bloom-forming cyanobacterium *Microcystis aeruginosa* to brackish water is driven by recent horizontal transfer of sucrose genes. Front. Microbiol. 9, 1150.
Te, S.H., Kok, J.W.K., Luo, R., You, L., Sukarji, N.H., Goh, K.C., Sim, Z.Y., Zhang, D., He, Y., Gin, K.YH., 2023. Coexistence of *Synechococcus* and *Microcystis* Blooms in a Tropical Urban Reservoir and Their Links with Microbiomes. Environ. Sci. Technol. 57 (4), 1613–1624.
Tee, H.S., Waite, D., Lear, G., Handley, K.M., 2021. Microbial river-to-sea continuum: gradients in benthic and planktonic diversity, osmoregulation and nutrient cycling. Microbiome 9 (1), 1–18.
Thees, A., Atari, E., Birbeck, J., Westrick, J.A., Huntley, J.F., 2019. Isolation and Characterization of Lake Erie Bacteria that Degrade the Cyanobacterial Microcystin Toxin MC-LR. J. Great. Lakes. Res. 45 (1), 138–149.
Tillett, D., Dittmann, E., Erhard, M., Do, H.Von, Neilan, B.A, 2000. Structural organization of microcystin biosynthesis in *Microcystis aeruginosa* PCC7806 : an integrated peptide polyketide synthetase system. Chem. Biol. 7 (10), 753–764.
Tonk, L., Bosch, K., Visser, P., Huisman, J., 2007. Salt tolerance of the harmful cyanobacterium Microcystis aeruginosa. Aquat. Microbial Ecol. 46, 117–123.
Tromas, N., Fortin, N., Bedrani, L., Terrat, Y., Cardoso, P., Bird, D., Greer, C.W., Shapiro, B.J., 2017. Characterising and predicting cyanobacterial blooms in an 8-year amplicon sequencing time course. ISME J. 11 (8), 1746–1763.
Tsuji, K., Setsuda, S., Watanuki, T., Kondo, F., Nakazawa, H., Suzuki, M., Harada, K., 1996. Microcystin levels during 1992–95 for lakes sagami and tsukui-japan. Nat. Toxins 4 (4), 189–194.
Tsuji, K., Watanuki, T., Kondo, F., Watanabe, M.F., Suzuki, S., Nakazawa, H., Suzuki, M., Uchida, H., Harada, KI., 1995. Stability of microcystins from cyanobacteria—II. Effect of UV light on decomposition and isomerization. Toxicon. 33 (12), 1619–1631.
Umehara, A., Tsutsumi, H., Takahashi, T., 2012. Blooming of *Microcystis aeruginosa* in the reservoir of the reclaimed land and discharge of microcystins to Isahaya Bay (Japan). Environ. Sci. Pollut. Res. 19, 3257–3267.
Verspagen, J.M.H., Passarge, J., Jöhnk, K.D., Visser, P.M., Peperzak, L., Boers, P., Laanbroek, H.J., Huisman, J., 2006. Water management strategies against toxic *Microcystis* blooms in the Dutch delta. Ecol. Appl. 16 (1), 313–327.
Waditee-Sirisattha, R., Ito, H., Kageyama, H., 2022. Global transcriptional and circadian regulation in a halotolerant cyanobacterium *Halothece* sp. PCC7418. Sci. Rep. 12 (1), 13190.
Wang, W., Sheng, Y., Jiang, M., 2022. Physiological and metabolic responses of *Microcystis aeruginosa* to a salinity gradient. Environ. Sci. Pollut. Res. 29 (9), 13226–13237.
Wang, Z., Liu, Y., Xu, Y., Xiao, P., Li, R., 2013. The divergence of cpcBA -IGS sequences between *Dolichospermum* and *Aphanizomenon* (Cyanobacteria) and the molecular detection of *Dolichospermum flos-aquae* in Taihu Lake, China. Phycologia 52 (5), 447–454.
Warnecke, F., Amann, R., Pernthaler, J., 2004. Actinobacterial 16S rRNA genes from freshwater habitats cluster in four distinct lineages. Environ. Microbiol. 6 (3), 242–253.
Warnecke, F., Sommaruga, R., Sekar, R., Hofer, J.S., Pernthaler, J., 2005. Abundances, identity, and growth state of actinobacteria in mountain lakes of different UV transparency. Appl. Environ. Microbiol. 71 (9), 5551–5559.
Wood, S.A., Crowe, A.L.M., Ruck, J.G., Wear, R.G., 2005. New records of planktonic cyanobacteria in New Zealand freshwaters. N.Z. J. Bot. 43 (2), 479–492.
Xu, Y., Wu, Z., Yu, B., Peng, X., Yu, G., Wei, Z., Wang, G., Li, R., 2008. Non-microcystin producing *Microcystis wesenbergii* (Komárek) Komárek (Cyanobacteria) representing a main waterbloom-forming species in Chinese waters. Environ. Pollut. 156 (1), 162–167.
Yancey, C.E., Smith, D.J., Den Uyl, P.A., Mohamed, O.G., Yu, F., Ruberg, S.A., Chaffin, J. D., Goodwin, K.D., Tripathi, A., Sherman, D.H., Dick, G.J., 2022. Metagenomic and metatranscriptomic insights into population diversity of *Microcystis* blooms: spatial and temporal dynamics of *mcy* genotypes, including a partial operon that can be abundant and expressed. Appl. Environ. Microbiol. 88 (9), e02464. -21.
Yuan, L., Zhu, W., Xiao, L., Yang, L., 2009. Phosphorus cycling between the colonial cyanobacterium *Microcystis aeruginosa* and attached bacteria, *Pseudomonas*. Aquat. Ecol. 43 (4), 859–866.
Zhang, C., Massey, I.Y., Liu, Y., Huang, F., Gao, R., Ding, M., Xiang, L., He, C., Wei, J., Li, Y., 2019. Identification and characterization of a novel indigenous algicidal bacterium *Chryseobacterium* species against *Microcystis aeruginosa*. J. Toxicol. Environ. Health, Part A 82 (15), 845–853.
Zhang, Y., Whalen, J.K., Cai, C., Shan, K., Zhou, H., 2023. Harmful cyanobacteria-diatom/dinoflagellate blooms and their cyanotoxins in freshwaters: a nonnegligible chronic health and ecological hazard. Water Res. 233, 119807.
Zheng, X., Wang, Y., Yang, T., He, Z., Yan, Q., 2020. Size-fractioned aggregates within phycosphere define functional bacterial communities related to *Microcystis aeruginosa* and *Euglena sanguinea* blooms. Aquatic Ecol. 54, 609–623.

Zhu, CM., Zhang, JY., Guan, R., Hale, L., Chen, N., Li, M., Lu, ZH., Ge, QY., Yang, YF., Zhou, JZ., 2019. Alternate succession of aggregate-forming cyanobacterial genera correlated with their attached bacteria by co-pathways. Sci. Total Environ. 688, 867–879.

Zhu, L., Zancarini, A., Louati, I., De Cesare, S., Duval, C., Tambosco, K., Bernard, C., Debroas, D., Song, L., Leloup, J., 2016a. Bacterial communities associated with four cyanobacterial genera display structural and functional differences: evidence from an experimental approach. Front. Microbiol. 7, 1662.

Zhu, L., Zuo, J., Song, L., Gan, N., 2016b. Microcystin-degrading bacteria affect *mcyD* expression and microcystin synthesis in *Microcystis* spp. J. Environ. Sci. 41, 195–201.

Zilliges, Y., Kehr, JC., Meissner, S., Ishida, K., Mikkat, S., Hagemann, M., Kaplan, A., Börner, T., Dittmann, E., 2011. The Cyanobacterial Hepatotoxin Microcystin Binds to Proteins and Increases the Fitness of *Microcystis* under Oxidative Stress Conditions. PLoS. One 6 (3), e17615.